Article:
Harvey, J, Garrido, C, Savov, IP et al. (5 more authors) (2014) 11B-rich fluids in subduction zones: the role of antigorite dehydration in subducting slabs and boron isotope heterogeneity in the mantle. Chemical Geology, 376. 20 - 30. ISSN 0009-2541

https://doi.org/10.1016/j.chemgeo.2014.03.015

^{11}B-rich fluids in subduction zones: the role of antigorite dehydration in subducting slabs and boron isotope heterogeneity in the mantle

Jason Harvey*[1], Carlos Garrido[2], Ivan Savov[1], Samuele Agostini[3], José Alberto Padrón-Navarta[4,5], Claudio Marchesi[2], Vicente López Sánchez-Vizcaíno[6], María Teresa Gómez-Pugnaire[2]

[1] School of Earth and Environment, University of Leeds, UK.

[2]Instituto Andaluz de Ciencias de la Tierra (IACT), CSIC & UGR, 18100 Armilla (Granada), Spain.

[3]Istituto di Geoscienze e Georisorse–CNR, Via Moruzzi 1, 56124 Pisa, Italy.

[4]Géosciences Montpellier, Univ. Montpellier 2 & CNRS, 34095 Montpellier, France.

[5]Research School of Earth Sciences, The Australian National University, Canberra 0200, ACT, Australia

[6]Departamento de Geología (Unidad Asociada al IACT-Granada), Escuela Politécnica Superior, Universidad de Jaén, 23700 Linares, Spain.

* Corresponding author. Telephone: +44 (0)113 343 6769. Fax: +44 113 343 5259. Email: feejh@leeds.ac.uk (J. Harvey).

For submission to Chemical Geology

Abstract

Serpentinites form by hydration of mantle peridotite and constitute the largest potential reservoir of fluid-mobile elements entering subduction zones. Isotope ratios of one such element, boron, distinguish fluid contributions from crustal versus serpentinite sources. Despite 85 % of boron hosted within abyssal peridotite being lost at the onset of subduction at the lizardite-to-antigorite transition, a sufficient cargo of boron to account for the composition of island arc magma is retained (c. 7 μg g^{-1}, with a $\delta^{11}B$ of +22 ‰) until the down-going slab reaches the antigorite-out isograd. At this point a ^{11}B-rich fluid, capable of providing the distinctive $\delta^{11}B$ signature of island arc basalts, is released. Beyond the uniquely preserved antigorite-out isograd in serpentinites from Cerro del Almirez, Betic Cordillera, Spain, the prograde lithologies (antigorite-chlorite-orthopyroxene-olivine serpentinite, granofels-texture chlorite-harzburgite and spinifex-texture chlorite-harzburgite) have very different boron isotope signatures ($\delta^{11}B$ = -3 to +6 ‰), but with no significant difference in boron concentration compared to the antigorite-serpentinite on the low P-T side of the isograd. ^{11}B-rich fluid, which at least partly equilibrated with pelagic sediments, is implicated in the composition of these prograde lithologies, which dehydrated under open-system conditions. Serpentinite-hosted boron lost during the early stages of dehydration is readily incorporated into forearc peridotite. This, in turn, may be dragged to sub-arc depths as a result of subduction erosion and incorporated in a mélange comprising forearc serpentinite, altered oceanic crust and pelagic sediment. At the antigorite-out isograd it dehydrates, thus potentially providing an additional source of ^{11}B-rich fluids.

52 **1. Introduction**

53

54 Nominally anhydrous, melt-depleted upper oceanic mantle accommodates very low
55 abundances of highly incompatible elements and volatiles (Salters and Stracke, 2004).
56 Serpentinization of refractory ultramafic lithologies hydrates peridotite (Seyfried and Dibble,
57 1980) and dramatically increases its cargo of fluid-mobile elements (As, Sb, B, Cs, Li, Pb, U,
58 Ba; e.g. Thompson and Melson, 1970; Bonatti et al., 1984; Benton et al., 2001; Savov et al.,
59 2005, 2007; Deschamps et al., 2011). For example, boron is easily incorporated into
60 serpentine phyllosilicates during serpentinization (Pabst et al., 2011) with boron
61 concentrations increasing by up to four orders of magnitude compared to anhydrous
62 peridotite (cf. Chaussidon and Jambon, 1994; Vils et al., 2008). Ultimately, serpentinites may
63 be subducted at convergent margins, potentially transporting their fluid-mobile element-,
64 halogen-, and noble gas-rich contents to sub-arc depths and beyond, hence introducing
65 volatile-rich fluid into arc magma sources upon dehydration and potentially generating
66 chemical and isotopic heterogeneity in the deeper convecting mantle (Scambelluri et al.,
67 1995; Benton et al., 2001; Savov et al., 2005, 2007; Sumino et al., 2010; Kendrick et al.,
68 2011, 2012).

69 Progressive dehydration of serpentinite, altered oceanic crust and pelagic sediment,
70 caused by compaction of pore space and low temperature dehydration reactions, releases
71 large volumes of pore fluid and structurally-bound water. An example of the consequences of
72 this early slab-fluid out-flux can be seen in the serpentinite mud volcanoes of the modern Izu-
73 Bonin-Mariana forearc (Fryer et al., 1985; Mottl, 1992; Fryer, 2011). Subduction-related
74 volcanism is controlled by deeper dehydration reactions which trigger and contribute to flux-
75 related melt generation in the overlying mantle wedge (e.g., Arculus and Powell, 1986;
76 Hattori and Guillot, 2003). Although this melting may be initiated by the introduction of slab-

derived fluids released by high P-T metamorphic devolatilization reactions (Schmidt and Poli, 1998), there is increasing evidence for fluid being generated by forearc serpentinite dragged down to sub-arc depths during subduction erosion (Savov et al., 2005; Tonarini et al., 2011; Marschall and Schumacher, 2012). Similarly, it is presently unclear whether the fluid is released continuously over a discrete interval (Schmidt and Poli, 1998; Kerrick and Connolly, 2001) or if it is released spasmodically in a series of pulses (Padrón-Navarta et al., 2010, 2011; John et al., 2012; Dragovic et al., 2012; Baxter and Caddick, 2013).

Irrespective of the mechanism governing the release of fluid, or its rate of release during dehydration, boron abundances and isotopes have been established as an excellent tracer for processes that involve flux-related melting at convergent margins (e.g. Bebout et al., 1993; Ryan and Langmuir, 1993; Tonarini et al., 2001). During dehydration reactions boron preferentially partitions into the fluid phase (Seyfried et al., 1984). Because of prior seawater-pelagic sediment interactions, boron is abundant in all of the lithologies that enter the trenches at subduction zones. However, how pelagic sediment, altered oceanic crust, and serpentinized peridotite (serpentinites) interact to produce the heterogeneous and somewhat ^{11}B-rich isotope signatures of arc volcanics remains equivocal. This ^{11}B-rich isotope signature of island arc volcanics, which extends to $\delta^{11}B = +18$ ‰ (where $\delta^{11}B$ refers to parts per thousand deviation in $^{11}B/^{10}B$ from NIST951 boric acid; Cantanzano et al., 1970) (Palmer, 1991; Ishikawa and Nakamura, 1994; Ishikawa et al., 2001; Tonarini et al., 2007, 2011), cannot be accounted for by fluid released from pelagic sediments ($\delta^{11}B$ of <0 ‰; [B] > 100 ppm; Ishikawa and Nakmura, 1993) or altered oceanic crust (mean $\delta^{11}B$ +3.4 ±1 ‰; mean [B] = 15 ppm; Smith et al., 1995). Although fluid-mineral fractionation releases fluids with ^{11}B-rich isotope signatures from these reservoirs at very shallow depths, deeper dehydration will only yield fluids with ^{11}B-poor isotope ratios (i.e. $\delta^{11}B$ <0 ‰; You et al., 1995; Peacock and Hervig, 1999; Benton et al., 2001; Marschall et al., 2006). Straub and Layne (2003)

suggest that a combination of altered oceanic crust and sediments is unlikely to produce a fluid, at sub-arc depths, with $\delta^{11}B$ of > +1 ‰. This is supported by the observation that not only is ^{11}B-rich fluid released by serpentinites in the forearc (Mottl, 1992; Savov et al. 2005, 2007), but also that a distinctly ^{11}B-poor signature remains in residual slab-hosted phengite, amphibole and epidote (Pabst et al., 2012). Seawater has a distinctive, ^{11}B-rich isotope signature ($\delta^{11}B$ c. +39.61 ±0.04 ‰; Foster et al, 2010) which is at least partially transferred to oceanic peridotite during the process of serpentinization at mid-ocean ridges (Boschi et al., 2008; Vils et al., 2009; Harvey et al., 2014), through fluid infiltration during slab bending at the outer rise of convergent margins (Ranero and Morgan, 2003; Ranero and Sallares, 2004; Faccenda et al., 2009), or through the hydration of forearc mantle overlying a slab undergoing subduction. This forearc serpentinite may be subsequently transported to sub-arc depths by subduction erosion (Hyndman and Peacock, 2003; Hattori and Guillot, 2007; Savov et al., 2007; Scambelluri and Tonarini, 2012). Even accounting for fluid-mineral fractionation under varying conditions of serpentinization, a range of ^{11}B-rich isotope ratios are preserved in serpentinized abyssal peridotite ($\delta^{11}B$ = +11.4 to +40.7 ‰; Boschi et al., 2008; Vils et al., 2009; Harvey et al., 2014), which potentially constitutes the largest component of the boron feedstock to the subduction factory.

All island arc volcanics are enriched in boron compared to the primitive mantle (cf. Chaussidon and Jambon, 1994; Ryan and Langmuir, 1993), but the evidence for how sufficient boron with a ^{11}B-rich signature is delivered to sub-arc depths to generate arc volcanics with $\delta^{11}B$ of up to +18 ‰ (Tonarini et al., 2007 and references therein) is not conclusive. This is because the series of hydration-dehydration reactions en route to the deep mantle suggests that much of the boron transported by slabs should be lost before sub-arc depths are attained (e.g. Kodolányi and Pettke, 2011). The aim of this study is to examine the boron elemental and isotopic signatures of natural samples that preserve a unique antigorite-

127 serpentinite to prograde chlorite-harzburgite isograd in the Cerro del Almirez, southern Spain
128 (Trommsdorff et al., 1998; Garrido et al., 2005; Padrón-Navarta et al., 2011). This unique
129 locality makes it an excellent natural laboratory for the examination of serpentinite
130 dehydration reactions at near sub-arc depths (680 to 710 °C and 1.6 to 1.9 GPa; Padrón-
131 Navarta et al., 2010). This study explores the significance of dehydration reactions in down-
132 going slabs at convergent margins and, specifically, evaluates the contribution these reactions
133 may (or may not) make to the production of ^{11}B-rich fluids implicated in arc-related
134 volcanism. In addition, we comment on the fate of boron retained within the prograde
135 lithologies and the likelihood that this boron may be implicated in the distinctive boron
136 systematics observed in ocean island basalts.
137
138 **2. Geological setting and sampling**
139
140 The Cerro del Almirez massif is one of several lenses of ultramafic material within
141 the upper sequences of the Nevado-Filábride Complex (Betic Cordillera Internal Zones,
142 Southern Spain; Figure 1). It comprises c. 2-3 km^2 of antigorite-serpentinite and chlorite-
143 harzburgite separated by a narrow (c.1 metre) zone of transitional lithologies (chlorite-
144 serpentinite and antigorite-chlorite-orthopyroxene-olivine serpentinite). The Nevado-
145 Filábride Complex experienced extensive metamorphism as a result of the Alpine orogeny
146 (Gómez-Pugnaire and Franz, 1988; Bakker et al., 1989; Puga et al., 1999), which peaked with
147 the subduction of serpentinites to eclogite-facies conditions during the Middle Miocene
148 (López Sánchez-Vizcaíno et al., 2001). The prograde transformation of antigorite-
149 serpentinite to chlorite-harzburgite occurred between 680 to 710 °C and 1.6 to 1.9 GPa
150 (Trommsdorff et al., 1998; Padrón-Navarta et al., 2010), where antigorite ceases to be a
151 stable phase and dehydration results in the formation of chlorite-bearing harzburgite. The

preserved P-T conditions are therefore consistent with eclogite-facies metamorphism at a depth of c. 50-60 km (Gerya and Yuen, 2003; Hacker et al., 2003). At Cerro del Almirez the chlorite-bearing harzburgite can be further subdivided according to texture, i.e. (a) granofels-texture chlorite-harzburgite with anhedral olivine and prismatic orthopyroxene (Padrón-Navarta et al. 2011) and (b) spinifex-texture chlorite-harzburgite with arborescent olivine and acicular orthopyroxene (e.g. Trommsdorff et al., 1998). Therefore, four distinctive Cerro del Almirez lithologies were sampled in order to investigate the effects of dehydration associated with eclogite-facies, subduction-related metamorphism; (i) antigorite-serpentinite, (ii) the "transitional lithologies" (in particular, antigorite-chlorite-orthopyroxene-olivine serpentinite), (iii) granofels-texture chlorite-harzburgite, and (iv) spinifex-texture chlorite-harzburgite. Representative samples of each of these lithologies are illustrated in e.g. Garrido et al. (2005), and Padrón-Navarta et al. (2011).

3. Analytical methods

Boron abundances and isotopic compositions were measured at IGG (CNR-Pisa, Italy) using a VG Isomass 54E positive ion thermal ionization mass spectrometer following boron extraction and purification procedures described by Tonarini et al. (1997, 2003). Briefly, following a K_2CO_3 alkali fusion, boron is extracted in ultra-pure water and purified using standard column chemistry. Boron is loaded onto Ta filaments as caesium borate prior to analysis by thermal ionisation mass spectrometry, where masses 309 and 310 represent ^{10}B and ^{11}B respectively. The $^{11}B/^{10}B$ isotopic ratio is reported in standard delta notation as per mil (‰) deviation from the mean value for the SRM951 boric acid standard (Cantanzaro et al., 1970) routinely passed through the same chemistry as the samples. Precision and accuracy are estimated conservatively as ± 0.64 ‰, based on replicate measurements of

177 reference material JB-2 ($\delta^{11}B$ = +7.25 ± 0.64 ‰ (2 σ), n=33 analyses with independent
178 chemistry).

179 Samples analysed for bulk rock Sr isotopes and Sr abundance were spiked using a
180 highly enriched ^{84}Sr solution before complete dissolution in Romil UpA HNO_3 and UpA HF,
181 prior to a final dissolution stage in 6M Romil UpA HCl. Strontium was extracted using Sr-
182 Spec resin in dilute UpA HNO_3, before drying prior to analysis by thermal ionisation mass
183 spectrometry (TIMS) at the University of Leeds on a Thermo Scientific Triton running in
184 static mode. The instrumental mass fractionation was corrected for by normalizing results to
185 $^{86}Sr/^{88}Sr = 0.1194$. The total Sr blank was negligible (< 100 pg) compared to the amount of
186 material processed (typically several hundred ng Sr). The analysis of SRM 987 standard
187 solution during the course of the measurements gave an average $^{87}Sr/^{86}$ Sr = 0.710248 ± 4
188 (2σ; n=11).

189

190 **4. Results**

191

192 Boron and strontium isotope ratios and elemental abundances were measured in
193 representative samples of each major lithological division (Table 1). Boron abundances range
194 from 7 to 12 μg g^{-1}, significantly higher than in primitive mantle estimates (0.25 μg g^{-1};
195 Chaussidon and Jambon, 1994), but much lower than in bulk-rock serpentinites from mid-
196 ocean ridge settings (mean [B] = 49 μg g^{-1}; Boschi et al., 2008; Vils et al., 2009), and mantle
197 wedge serpentinites (mean [B] c. 20 μg g^{-1}; Benton et al., 2001; Savov et al., 2007;
198 Scambelluri and Tonarini, 2012). Antigorite-serpentinite and granofels-texture chlorite-
199 harzburgite contain the lowest boron abundances (7.03 and 7.15 μg g^{-1} respectively; Figure
200 2), while the transitional lithologies contain the most boron (11.78 μg g^{-1}). Two
201 measurements of [B] in spinifex-texture chlorite-harzburgite gave abundances of 7.59 and

10.34 μg g^{-1}. Boron isotope ratios are also highly variable ($\delta^{11}B$ = +25.07 ± 1.68 ‰ to -3.46 ± 0.27 ‰). With a range of $\delta^{11}B$ from +21.61 to +25.07 ‰, antigorite-serpentinite is indistinguishable from $\delta^{11}B$ of serpentinites recovered from the Mid-Atlantic Ridge (Boschi et al., 2008; Vils et al., 2009; Harvey et al., 2014), and convergent margins (Benton et al., 2001; Tonarini et al., 2007; Scambelluri and Tonarini, 2012). In particular, $\delta^{11}B$ in the Cerro del Almirez serpentinites falls between the values of abyssal serpentinites from the Atlantis Massif ($\delta^{11}B$ = +11.38 to +15.15 ‰, Boschi et al., 2008) and ODP Leg 209 (15° 20´ Fracture Zone, Mid Atlantic Ridge; $\delta^{11}B$ =+29.72 to +40.66 ‰, Vils et al., 2009). All other lithologies have significantly lower $\delta^{11}B$ (≤ +6.2 ‰), with spinifex-texture chlorite-harzburgite ranging from +2.68 ± 0.35 ‰ to +6.22 ± 0.76 ‰, transitional lithologies having $\delta^{11}B$ of +3.38 ± 0.35 ‰, and granofels-texture chlorite-antigorite $\delta^{11}B$ values of -3.3 ± 0.27 ‰.

Strontium elemental abundance is consistently <10 μg g^{-1}, while $^{87}Sr/^{86}Sr$ ranges from 0.70752 ± 1 to 0.70871 ± 2, i.e. significantly more radiogenic than depleted MORB-source mantle (e.g. Pacific MORB glass mean $^{87}Sr/^{86}Sr$ = 0.7026, n= 602; http://www.petdb.org; Lehnert et al., 2000) and approaching the value for modern-day seawater ($^{87}Sr/^{86}Sr$ = 0.70916; Palmer and Edmond, 1989). In general, the Sr isotope ratios of the antigorite-serpentinite, the antigorite-chlorite-orthopyroxene-olivine transitional lithology, and the granofels-texture chlorite harzburgite are remarkably similar ($^{87}Sr/^{86}Sr$ = 0.70819 ± 1 to 0.70871 ± 2), with this entire range being found within the antigorite-serpentinite alone. In contrast, Sr elemental abundance is variable across these lithologies. The antigorite-chlorite-orthopyroxene-olivine transitional lithology has a higher [Sr] (4.33 μg g^{-1}) than both the antigorite-serpentinite ([Sr] = 0.33 to 2.29 μg g^{-1}) and the prograde granofels-texture chlorite-harzburgite ([Sr] = 1.23 μg g^{-1}). Curiously, the highest [Sr] of all the lithologies is found in the prograde spinifex-texture chlorite-harzburgite ([Sr] = 5.57 to 9.50 μg g^{-1}) which is accompanied by a much less radiogenic Sr isotope ratio ($^{87}Sr/^{86}Sr$ = 0.70752 ± 1 to 0.70763 ±

1). All of the Cerro del Almirez lithologies are significantly more radiogenic than similar serpentinites reported by e.g. Scambelluri and Tonarini (2012), where $^{87}Sr/^{86}Sr$ ranges from 0.704584 to 0.706520, and more closely resemble Mid-Atlantic Ridge serpentinites whose $^{87}Sr/^{86}Sr$ ranges from 0.707318 to 0.70921 for both leached and unleached serpentinites (Boschi et al., 2008; Vils et al., 2009; Harvey et al., 2014). The $^{87}Sr/^{86}Sr$ of the Cerro del Almirez samples are also indistinguishable from modern day vent fluids recovered from the Logatchev hydrothermal field ($^{87}Sr/^{86}Sr$ = 0.70394 to 0.70914; Amini et al., 2008).

5. Discussion

Elements which preferentially partition into a fluid phase during dehydration will become strongly depleted in the prograde assemblage (Bebout et al., 1993) and, in the case of boron in particular, the potential exists for a strong fractionation of boron isotopes given favourable temperature and *p*H conditions. The drastic shift in $\delta^{11}B$ observed at Cerro del Almirez during the transformation of antigorite-serpentinite, first to the transitional lithologies, and subsequently to the chlorite-bearing harzburgites, is consistent with this prediction and the production of ^{11}B-rich fluids. However, both boron and strontium abundances in the prograde lithologies are difficult to reconcile with a simple dehydration reaction that results in a loss of boron and strontium while fractionating boron isotope ratios. This is compounded by an unusually low loss of fluid at the antigorite-out isograd, based upon loss on ignition (LOI) values for the Cerro del Almirez lithologies (Figure 2; cf. Scambelluri et al., 2001, 2004). These observations suggest that a completely closed-system transformation from antigorite-serpentinite to chlorite-harzburgite may not have occurred. As such, it is necessary to (i) examine the nature of the protolith and (ii) confirm that the Cerro del Almirez represents an isograd in the field, i.e. ensure that the observed field relations are

not consistent with a tectonic contact, (iii) examine the degree to which the Cerro del Almirez antigorite-serpentinite to chlorite-harzburgite transition remained isochemical, i.e. a closed system during metamorphism, and (iv) quantify the effects of boron release from the downgoing antigorite-serpentinite.

5.1. The formation and composition of the antigorite-serpentinite protolith

Serpentinization of a nominally anhydrous ultramafic precursor, either at a mid-ocean ridge (e.g. Bach et al., 2004), or as a result of flexure when a lithospheric plate enters a subduction zone (e.g. Ranero et al., 2003), has the effect of transforming an olivine-pyroxene-dominated lithology into lizardite (and / or chrysotile) phyllosilicates which contain c. 12 wt. % H_2O ("serpentinization *sensu stricto*"; e.g., Miyashiro et al., 1969; Wicks and Whittaker, 1977; Komor et al., 1985; Janecky and Seyfried, 1986; O'Hanley, 1996) and develop fluid-mobile element abundances orders of magnitude higher than their anhydrous precursor. Although it can be challenging to distinguish between serpentinites derived from mantle wedge and those originating from subducted oceanic lithosphere (e.g. Hattori and Guillot, 2007; Deschamps et al., 2013), the ultramafic lithologies of Cerro del Almirez have been identified as being the result of seafloor serpentinization. This origin is supported by the ratio of SO_4 to total sulphur and S-D-H-O isotope signatures (Alt et al., 2012). In addition, a comparison of the trace element abundances and, in particular, the high abundances of relatively immobile heavy rare earth elements of Cerro del Almirez antigorite-serpentinites compared to subducted serpentinites (cf. Marchesi et al., 2013; Deschamps et al., 2013) illustrates that the latter is the most likely precursor lithology.

Soon after the onset of subduction, lizardite is no longer stable and will be transformed to the high(er) temperature serpentine variant, antigorite, at 200-400 °C; (Evans

et al., 1976; Ribeiro da Costa et al., 2008; Kodolányi and Pettke, 2011; Schwartz et al., 2013). Critically, this is expected to be accompanied by B depletion (84 ± 5 %; Scambelluri et al., 2004; Savov et al., 2007; Deschamps et al., 2010; Kodolányi and Pettke, 2011; Vils et al., 2011) and a significant loss of Sr (50 ± 40 %; Kodolányi and Pettke, 2011). The Cerro del Almirez antigorite-serpentinite is indeed depleted in Sr compared to lizardite-rich abyssal peridotites, containing only around 15 % of the Sr budget of lower P-T serpentinites (Marchesi et al., 2013). Boron is also significantly depleted in the Cerro del Almirez antigorite-serpentinite. Compared to abyssal serpentinites with a mean boron concentration of 45 μg g^{-1} (Deschamps et al., 2013) the antigorite-serpentinites of this study ([B] = 7 μg g^{-1}) have lost approximately 85 % of their B budget at the onset of subduction (Figure 3). Abundances of Cs, U and Rb are also moderately depleted in Cerro del Almirez antigorite-serpentinites compared to mantle wedge and abyssal serpentinites (Figure 3), as suggested by their mobility in subduction zone fluids elsewhere (Savov et al., 2007).

The ^{11}B-rich signature of Cerro del Almirez antigorite-serpentinite ($\delta^{11}B$ = +22 to +25 ± 2 ‰) falls within the reported range of abyssal serpentinites ($\delta^{11}B$ = +11.4 to +40.7; Boschi et al., 2008; Vils et al., 2009; Harvey et al., 2014). This suggests that the loss of B, during the shallow lizardite to antigorite transition, may not have been accompanied by significant fluid-mineral fractionation of B isotopes, although small amounts of fractionation are difficult to recognize, given the large range of $\delta^{11}B$ in abyssal serpentinites. Therefore, the $\delta^{11}B$ of the abyssal serpentinite protolith prior to subduction was probably retained with the formation of antigorite. This hypothesis is supported by the observation that early metamorphism during subduction occurs in the presence of a high *p*H fluid, which does not fractionate isotopes of boron during fluid-assisted metamorphism at c. 300 °C (Mottl et al., 1992; Savov et al., 2005, 2007; Foustoukos et al., 2008).

302 *5.2 Metamorphic isograd versus tectonic contact*

303

304 The dramatic change in $\delta^{11}B$ coupled with little or no loss of boron (and even an
305 increase in [B]) across the antigorite-out isograd isograd could be explained if the boundaries
306 between the lithologies at Cerro del Almirez were faulted contacts rather than the result of
307 continuous dehydration of antigorite-serpentinite (Figure 2). However, there is no field
308 evidence to support this hypothesis, i.e. evidence for truncated structures, mylonites or
309 cataclasis is lacking (Morten and Puga, 1984; Trommsdorff et al., 1998; Padrón-Navarta et
310 al., 2011). In addition, the sequence of reactions and progressive changes in mineralogy
311 observed in the field during the transition from antigorite-serpentinite, through chlorite-
312 serpentinite and antigorite-chlorite-orthopyroxene-olivine-bearing assemblages (the
313 transitional lithologies), to chlorite-harzburgites are consistent with the results of piston
314 cylinder experiments designed to mimic the effects of progressive fluid loss during the
315 dehydration of a cold slab (Padrón-Navarta et al., 2010). Increasing P-T conditions replicated
316 the mineralogical assemblages observed on the high P-T side of the isograd using an
317 antigorite-serpentinite starting assemblage (Padrón-Navarta et al., 2010).

318 Moreover, textural relationships, mineral compositions and chemographic phase
319 relations indicate that the prograde breakdown of antigorite-serpentinite to chlorite-
320 harzburgite occurred through a series of continuous metamorphic reactions forming the
321 intervening transitional lithologies of the Cerro del Almirez (Padrón-Navarta et al., 2011).
322 Although the earlier study of Trommsdorff et al. (1998) did not recognize transitional
323 lithologies and reported a sharp contact between antigorite-serpentinite and chlorite-
324 harzburgite (the "antigorite-out" isograd), this earlier work also came to the conclusion that
325 the change in mineralogy observed is consistent with dehydration of an antigorite-rich
326 precursor rather than the contrasting lithologies being juxtaposed as a result of tectonism. The

more recent observations of Padrón-Navarta et al. (2011), coupled with experimental evidence determining the nature of the transitional lithologies, overlooked in previous studies (Trommsdorff et al., 1998; Hürlimann, 1999; Schönbächler, 1999; Garrido et al., 2005), only strengthens this hypothesis. Critically, the antigorite-serpentinite to chlorite-serpentinite lithological transition is oblique to and overprints the penetrative foliation of the antigorite-serpentinite (see Figure 4a and b in Padrón-Navarta et al., 2011). This indicates that chlorite-serpentinite formed at the expense of a foliated antigorite-serpentinite protolith similar to those overlying the transitional lithologies.

5.3 Open versus closed system dehydration

Major element compositions do not radically alter during dehydration (Padrón-Navarta et al., 2011; Marchesi et al., 2013; Figure 4) and the bulk composition of the protolith is largely preserved. However, changes in trace element abundances during the metamorphic sequence suggest that the transformation of antigorite-serpentinite to chlorite-harzburgite cannot have occurred as part of a closed system (Figure 5; Garrido et al., 2005; Marchesi et al., 2013) and that the non-isochemical transformations may shed some light on the $\delta^{11}B$ systematics and boron abundances that are otherwise difficult to interpret. A large change in $\delta^{11}B$, from +22 ‰ to +3 ‰, occurs as antigorite-serpentinite transforms to the transitional lithologies. Fluid-mineral fractionation of boron isotopes, controlled by the temperature and the *p*H of the fluid involved is common (e.g. Boschi et al., 2008; Harvey et al., 2014). Since the transition between these two lithologies constitutes a dehydration reaction, it is not surprising that a sharp change in boron isotope ratios is observed between the antigorite-serpentinite and the transitional lithologies. Indeed the release of a fluid enriched in ^{11}B is required to account for the $\delta^{11}B$ of arc volcanics, which extend to values of

352 $\delta^{11}B$ ~ +18 ‰ (Tonarini et al., 2011). However, despite the likelihood of the release of a ^{11}B-
353 rich fluid, simple dehydration and the loss of a ^{11}B-bearing fluid cannot account for the
354 observed composition of the prograde lithologies.

355 For example, the transitional lithologies are richer in both B and Sr than the
356 antigorite-serpentinite and differ in terms of bound H_2O, represented by loss on ignition, by
357 less than 0.5 wt %. In fact the transitional lithologies are richer in many of the incompatible
358 trace elements compared to the antigorite-serpentinite pre-cursor (Figure 5). It is difficult to
359 account for the shift in observed isotope ratios with little net change in the boron elemental
360 budget and the relatively high Sr abundances observed in the transitional lithologies. Given
361 that the transitional lithologies are relatively enriched not only in fluid-mobile elements (B,
362 Cs, Ba, Rb, Sr), but also some high field strength elements (Nb, Ta) (Figure 3), externally
363 derived fluids, i.e. not associated with the dehydration of antigorite-serpentinite, may have
364 metasomatized the prograde lithologies. In other words, the B and Sr isotope signature of the
365 prograde lithologies is unlikely to solely reflect the process of dehydration at the antigorite-
366 out isograd. Indeed, Marchesi et al. (2013) calculated that up to 40 m^3 of external fluids
367 equilibrated with crustal sources fluxed through each cubic metre of dehydrated chlorite-
368 harzburgite. Although elevated to levels significantly above those of other similar
369 serpentinites (cf. Scambelluri and Tonarini, 2012), the Nb/B ratios from Cerro del Almirez
370 are remarkably similar to those of arc lavas in general (Figure 6).

371 Partial equilibration with a crustally derived, Sr-rich fluid may have not only added Sr
372 (and Nb) to a protolith that originally resembled Mid-Atlantic Ridge serpentinite (typically <
373 2ppm Sr, $^{87}Sr/^{86}Sr$ up to 0.70921; Paulick et al., 2006; Harvey et al., 2014) but also affected
374 its Sr isotope ratio. Whether or not the serpentinites of Scambelluri and Tonarini (2012)
375 preserve $^{87}Sr/^{86}Sr$ that is typical of subducted serpentinites ($^{87}Sr/^{86}Sr$ = 0.704584 to 0.706520)
376 is difficult to assess, given the wide range of Sr isotope ratios preserved both at mid-ocean

ridges and in subducted serpentinites. What is clear from the study of Logatchev hydrothermal fluid by Amini et al. (2008) is that local variations in Sr isotope ratio through interaction with an externally derived fluid can vary enormously ($^{87}Sr/^{86}Sr$ = 0.70394 to 0.70914). Furthermore, at least some of the Sr isotope signature of oceanic serpentinites is derived from an easily leachable component (Harvey et al., 2014), making the significance of the Sr isotope ratios of this study difficult to interpret in the context of closed system dehydration. An alternative explanation for the remarkable differences in incompatible trace element abundances of the prograde lithologies is that they did not share a common protolith. However, as outlined in section 5.2 above, and explored in detail in Padon-Navarta et al. (2010) and Marchesi et al. (2013), the mineralogical changes observed in the prograde lithologies are consistent with the Cerro del Almirez antigorite serpentinite being the protolith of all of the prograde lithologies.

Given the enrichment of the prograde lithologies in high field strength elements and some of the fluid-mobile elements, and the relative loss of rare earth elements, a non-isochemical evolution to the chlorite-harzburgite lithologies also seems likely (Marchesi et al., 2013; Figures 3, 4 and 5). Moreover, the compositions of the two chlorite-harzburgite lithologies are difficult to explain through interaction with a single fluid external to the dehydration process. For example, the $\delta^{11}B$ and $^{87}Sr/^{86}Sr$ of the two chlorite-harzburgites differ significantly (Table 1). The granofels textured chlorite-harzburgite ($\delta^{11}B$ = -3.4 ‰; $^{87}Sr/^{86}Sr$ = 0.70820) has a less ^{11}B-rich and more radiogenic Sr isotope signature than the spinifex-texture chlorite-harzburgite ($\delta^{11}B$ = + 2.7 to + 6.2 ‰; $^{87}Sr/^{86}Sr$ = c. 0.7076). The latter lithology also contains by far the most Sr of all of the lithologies analysed ([Sr] = 5.57 to 9.50 $\mu g\ g^{-1}$), which is difficult to reconcile with the observation elsewhere that Sr is lost as a result of subduction-related dehydration (e.g. Kodolányi and Pettke, 2011). This is, however, consistent with the observation of Savov et al. (2005) where changes in Sr

systematics of arc volcanics can be related to changes in fluid composition beneath the arc. The favoured models of Padrón-Navarta et al. (2011) for the formation of the different prograde lithologies (spinifex- versus granofels-texture chlorite-harzburgite) involve the pulsed release of fluids to account for their mineralogical and chemical composition, not unlike the hypothesis of Fryer et al. (2006) to account for the distribution of serpentinite muds in the modern-day Izu-Bonin-Marianas arc. The association of spinifex-texture chlorite-harzburgite with Sr and B isotope systematics that differ from the granofels-texture chlorite-harzburgite suggests that two fluids with different compositions were present. This is supported by the observations that fluids that had equilibrated with sediments ($\leq$ -5 ‰; Ishikawa and Nakmura, 1993), as suggested by Marchesi et al. (2013), would possess a particularly low $\delta^{11}B$ (Tonarini et al., 2011). Indeed, more than one fluid is also required to account for the composition of modern-day Izu-Bonin-Mariana arc volcanics (Ishikawa and Tera, 1999). In summary, it would appear that while there is strong chemical and isotopic evidence for the antigorite-serpentinite retaining the characteristics of a hydrated serpentinite that passed through the lizardite-to-antigorite transition beneath the forearc, it is difficult to reconcile the B and Sr elemental and isotopic characteristics of the prograde lithologies with subduction-related dehydration alone. Either they lost the majority of their boron during metamorphism and acquired a subsequent metasomatic overprint from a fluid unrelated to subduction or, more likely, the influx of a fluid not related to antigorite breakdown was involved during fluid-assisted dehydration of antigorite-serpentinite (Ishikawa and Tera, 1999; Kodolányi and Pettke, 2011).

5.4 Slab serpentinite versus entrained forearc serpentinite as a source of the $\delta^{11}B$ signature of arc volcanics

427 Notwithstanding the uncertainty of the source of the B and Sr elemental and isotopic
428 signatures of the prograde lithologies at Cerro del Almirez, the composition of the antigorite-
429 serpentinite prior to subduction-related dehydration provides valuable information regarding
430 the cargo of fluid mobile elements going into the dehydration reaction and, critically, their
431 capacity for contributing to the distinctive signature of arc volcanics. However, portions of
432 serpentinized forearc wedge can also be transported to similar depths as the Cerro del
433 Almirez antigorite-serpentinites through subduction erosion (e.g. Tonarini et al., 2011;
434 Marschall and Schumacher, 2012; Scambelluri and Tonarini, 2012), and this forearc wedge
435 has the capacity to carry a large cargo of B with a high and variable $\delta^{11}B$, acquired during the
436 addition of fluid mobile elements in the forearc (Benton et al., 2001; Savov et al. 2005, 2007;
437 Pabst et al., 2011; Kodolányi and Pettke, 2011). Thus, instead of its derivation from the
438 dehydration of a subducting slab, an alternative means for the delivery of ^{11}B-rich fluid to the
439 sub-arc portion of the mantle wedge may come from forearc serpentinites entrained during
440 subduction erosion. If 85 ± 5 % of the original boron cargo of a portion of subducted
441 serpentinite is lost during the transition from lizardite- to antigorite-serpentinite (Savov et al.,
442 2007; Kodolányi and Pettke, 2011; this study), the vast majority of boron available for
443 transfer at depth into the source region of arc volcanics has already been lost from the slab
444 and most likely transferred into this shallow part of the overlying mantle wedge.
445 The recent comprehensive review of subducted serpentinites by Deschamps et al.
446 (2013) demonstrates that there is a large degree of scatter in the available data from
447 individual tectonic settings. However, despite these limitations, the boron abundance and
448 isotopic characteristics of Cerro del Almirez lithologies (Scambelluri et al., 2004; this study)
449 represent those of the only known antigorite-serpentinite at the cusp of dehydration, i.e.
450 immediately adjacent to the antigorite-out isograd. Its categorization as a portion of
451 subducted slab (Alt et al., 2012; Marchesi et al., 2013) places it beneath the subduction

452 channel (Gerya et al., 2002; King et al., 2003) during active subduction. On the other hand,
453 serpentinite mud and clasts recovered during Ocean Drilling Program Legs 125 and 195 from
454 the modern Izu-Bonin-Mariana forearc (Benton et al., 2001) represent modern day forearc
455 serpentinites, hydrated during the early dehydration of abyssal peridotites, altered oceanic
456 crust and pelagic sediments, which have been entrained by the down-going slab and
457 subsequently exhumed along the subduction channel (e.g. Savov et al., 2005, 2007, Pabst et
458 al., 2012). Using these end-members a quantitative assessment of the relative contribution to
459 the boron budget of arc volcanoes from the slab versus fore-arc serpentinite can be attempted.
460 Island arc basalts have a wide range of boron isotope values ($\delta^{11}B$ up to +18 ‰) and
461 boron abundances ([B] up to 90 μg g^{-1}, but more typically c. 15 μg g^{-1}; Ryan and Langmuir,
462 1993; Tonarini et al., 2007, 2011). A mantle wedge domain that melts to produce island arc
463 basalt must have similar isotopic characteristics to the melt it produces, since isotope ratios
464 are barely fractionated at magmatic temperatures. Transfer of boron to the mantle wedge as a
465 result of dehydration, followed by a simple batch melting calculation can be employed to
466 ascertain whether the boron budget of the Cerro del Almirez antigorite-serpentinite is capable
467 of providing an adequate feedstock of fluid-mobile boron into the overlying mantle wedge,
468 that will subsequently be incorporated into island arc basalts. The boron abundance of the
469 antigorite-serpentinite in this study is 7 μg g^{-1}, and using the experimentally determined fluid
470 / residue partition coefficient of Tenthorey and Herman (2004), i.e. D = 4, it can be assumed
471 that 80 % of the boron content of the antigorite-serpentinite will be lost during dehydration;
472 the remaining 20 % being retained in the down-going prograde assemblage. Fluid loss as a
473 result of the production of the transitional lithologies and prograde assemblages at the
474 expense of antigorite-serpentinite is between 2.8 and 3.3 weight % (Marchesi et al., 2013).
475 The fluid produced has a B/H_2O ratio of 2.5 x 10^{-5} to 4.2 x 10^{-5}. As boron and water are
476 almost perfectly incompatible during partial melting of the mantle (Brenan et al., 1998) this

ratio is expected to be preserved when the mantle wedge undergoes partial melting (assuming that both its boron and water contents were negligible to start with). Using $C_l = C_o/[D\text{-}F(1\text{-}D)]$, where C_l is the [B] in the melt produced, C_o is the [B] lost from Cerro del Almirez antigorite-serpentinite during dehydration i.e., 5.6 μg g^{-1} (80 % of the 7 μg g^{-1} abundance measured in the antigorite-serpentinite) and provides the boron feedstock for any subsequent melting, D is the bulk rock partition coefficient during partial melting ($D_B^{\text{bulk rock/melt}}$ = 0.003 to 0.02; Brenan et al., 1998) and F is the fraction of partial melting (15 to 30 % melt production in arc settings; Pearce and Parkinson, 1993) will yield [B] in island arc volcanics of 18 to 37 μg g^{-1}, i.e. well within the range of [B] observed at actual island arc settings. However, several assumptions need to be made for this calculation to be valid. First of all, the mantle wedge protolith (i.e. pre-hydration) has a composition resembling asthenospheric mantle ($\delta^{11}B$ = -10 ‰; Chaussidon & Marty, 1995; [B] 0.25 μg g^{-1}; Chaussidon & Jambon, 1994), i.e. a composition that is instantly overprinted by the first influx of boron-rich fluid with a high ^{11}B content. Secondly, this assumes that all of the boron lost from antigorite-serpentinite at the antigorite-out isograd is transferred to the overlying mantle wedge. This is difficult to assess quantitatively as the prograde lithologies from this study are assumed to have metamorphosed under open-system conditions, i.e. it is not possible to determine what proportion, if any, of the original boron budget was actually retained at the isograd and what was added under open-system conditions, although the use of the experimentally determined fluid / residue partition coefficient of Tenthorey and Hermann (2004) does allow this to be at least partially constrained. Finally, it assumes that there is a constant-rate loss of boron from the mantle wedge through the production of melt (constant volcanic output at arc fronts) and steady-state supply of boron to the mantle wedge (constant rate of subduction of uniformly serpentinized material), i.e. there is no opportunity for boron either to be completely exhausted from the mantle wedge undergoing partial melting, or to accumulate to such

extents that boron concentrations can become particularly enhanced during a period of magmatic quiescence.

While some of these assumptions are not critical to the overall result of the calculation, others do have an effect on the range of compositions of arc magmas. The transfer of the boron cargo from Cerro del Almirez antigorite-serpentinite to arc basalts, first by dehydration and then by melting does not replicate the entire range of [B] observed in arc volcanics. However, mean subducted serpentinite (Deschamps et al., 2013) has a [B] of c. 23 $\mu g\ g^{-1}$, and using this value in the simple batch melting calculation produces a range of B concentrations of 59 to 121 $\mu g\ g^{-1}$, which easily encompasses the upper range of [B] observed at island arcs. The almost perfect incompatibility of boron during fractional crystallization will also ensure that magmatic differentiation further concentrates B in the remaining melt (Tonarini et al., 2011). Moreover, B/H_2O remains invariant during the partial melting of hydrated mantle wedge. This is supported by the observation that the calculated B/H_2O ratios for fluid released from Cerro del Almirez are indistinguishable from the composition of island arc-derived melt inclusions (modified MORB source melt inclusions, Bouvier et al., 2008). Finally, binary mixing of serpentine-derived fluid with fluid in equilibrium with marine sediments (mean $\delta^{11}B$ = -4 ‰, mean [B] = 115 $\mu g\ g^{-1}$; Ishikawa and Nakamura, 1993), would be able to account for the full compositional range of island arc volcanics presented in previous studies (e.g. Ryan and Langmuir, 1993; Tonarini et al., 2007, 2011; Scambelluri and Tonarini, 2012) and is also consistent with the hypothesis of Ishikawa and Tera (1999) that requires two distinctly different fluids to account for many island arc compositions.

However, fluid produced by dehydration in the slab must cross the subduction channel (Gerya et al., 2002; King et al., 2003) before it reaches the overlying mantle wedge. An alternative hypothesis for the source of fluid delivered to the arc magma source region is

527 serpentinite / altered oceanic crust / marine sediment mélanges dragged to comparable depths
528 to the antigorite-out isograd through subduction erosion, along the subduction channel,
529 directly above the subducting slab (Savov et al., 2007; Marschall and Schumacher, 2012).
530 The combination of this mélange and abundant chlorite ± actinolite-schist (Ukar, 2012; Ukar
531 et al., 2012), produced from the intimate association of ultramafic and mafic lithologies,
532 contains as much fluid as the down-going slab itself (Spandler et al., 2008; Pabst et al., 2012;
533 Marschall and Schumacher, 2012). This assemblage is also likely to be boron-rich;
534 Deschamps et al. (2013) report [B] for mantle wedge serpentinites of 22 to 72 μg g^{-1}.
535 Moreover, a mélange contains all of the hydrated lithologies required to fulfil the
536 requirements of the two-fluid hypothesis of Ishikawa and Tera (1999). As demonstrated by
537 the calculations above, the supply of all of the fluid from both the dehydrating slab and the
538 overlying mélange is not required to account for the composition of island arc basalts. There
539 is sufficient availability and mobility of B in either reservoir for the reproduction of the
540 typical range of compositions measured in arc basalts. Accordingly, the basalts may result
541 from either dehydration of mélange overlying the down-going slab, the down-going slab
542 itself, or a combination of the two. Given that the slab is separated from the mantle wedge by
543 the mélange and strongly foliated chlorite-schist that bounds the subduction channel
544 (Marschall and Schumacher, 2012), the passage of slab-derived fluid may be impeded, but
545 the exact provenance of the fluid responsible for enriching mantle wedge, i.e. the source of
546 island arc fluid-mobile element budgets, remains equivocal.
547
548 *5.5 The fate of boron in prograde lithologies – asthenospheric heterogeneity?*
549
550 Irrespective of the exact mechanism of antigorite-serpentinite dehydration, i.e. open-
551 versus closed-system, the overall result of the antigorite-serpentinite to chlorite-harzburgite

552 transition is incomplete dehydration, i.e. 5 to 6 wt. % of H_2O remains in the prograde
553 lithologies at Cerro del Almirez (Padrón-Navarta et al., 2011). This means that the potential
554 exists for the delivery of volatiles (Kendrick et al., 2011), boron and other fluid-mobile
555 elements (and a wide range of other variably mobile elements; Morris and Ryan, 2003) to
556 much greater depths than those associated with flux melting of sub-arc mantle wedge. While
557 hydrous chlorite may be abundant (exceptionally, up to 20 modal %) in the Cerro del Almirez
558 prograde assemblage (Alt et al., 2012), the contribution to the boron budget from chlorite is
559 low compared to other phases (chlorite mean [B] = 5 $\mu g\ g^{-1}$, Scambelluri et al., 2004; Pabst et
560 al., 2012; Figure 7), e.g. prograde olivine, present as at least 40 modal % in harzburgite, by
561 definition (mean prograde olivine [B] = 38 $\mu g\ g^{-1}$, Scambelluri et al., 2004; Figure 7). Brine-
562 rich fluid inclusions, abundant in brown and colourless prograde olivine (Scambelluri et al.,
563 2004; Padrón-Navarta et al., 2011), are the dominant hosts of B in the prograde assemblage,
564 with B abundances up to two orders of magnitude greater than that of chlorite (Figure 7). If
565 the prograde lithologies sampled at Cerro del Almirez survive further dehydration beneath
566 and beyond the arc - prograde olivine is an anhydrous phase (notwithstanding its fluid-
567 inclusion content) - it is possible that peridotite that is significantly enriched in boron, and
568 with a heterogeneous $\delta^{11}B$ may be returned to the convecting mantle. This in turn may have
569 implications for the generation of the wide range of compositions observed in ocean island
570 basalts.
571
572 **6. Concluding remarks**
573
574 The prograde lithologies on the high P-T side of the antigorite-out isograd at Cerro del
575 Almirez are complex and likely preserve evidence not only for the dehydration of antigorite-
576 serpentinite but also the flux of fluids partially equilibrated with pelagic sediment.

577 Notwithstanding the complexities of the prograde lithologies, the antigorite-serpentinite on
578 the low P-T side of the antigorite-out isograd appears to preserve the composition of
579 subducted serpentinite prior to dehydration at pressures and temperatures of 1.6 to 1.9 GPa
580 and 680 to 710 °C. This allows a quantitative assessment of the possibility that slab-hosted
581 antigorite-serpentinite is a significant source of fluid-mobile elements delivered to the
582 overlying mantle wedge, which are subsequently incorporated in island arc volcanics.
583 Assuming the removal of 80 % of the boron from the antigorite-serpentinite at the antigorite-
584 out isograd, and its transfer into the overlying mantle wedge, subsequent partial melting of
585 this boron-enriched reservoir is capable of producing the range of boron abundances observed
586 in island arcs. With the influence of pelagic sediments, or fluids derived from them, the full
587 range of isotopic and elemental characteristics of island arc basalts can be produced with
588 simple batch melting and mixing calculations. However, the dehydrating slab is separated
589 from the overlying wedge by the subduction channel and possibly mélange, comprising
590 serpentinite eroded from the fore-arc (dragged to the antigorite-out isograd during subduction
591 erosion), altered oceanic crust, and pelagic sediment. The boron elemental flux and isotopic
592 signature of such a mélange should not differ significantly from that of slab derived fluids
593 and, as such, may also constitute a source of fluids which hydrate the overlying mantle wedge
594 and form the source for island arc basalts. Distinguishing between these two sources of fluids
595 (slab versus mélange) remains problematic.

596 The prograde lithologies on the high P-T side of the antigorite-out isograd have much
597 lower $\delta^{11}B$ signatures but still contain a comparable cargo of boron to antigorite-serpentinite.
598 This is because they have at least partly equilibrated with pelagic sediment-derived fluids.
599 The preservation, in the prograde lithologies, of boron in olivine-hosted fluid inclusions
600 allows the transport of boron, with a higher $\delta^{11}B$ than primitive mantle, to depths below that
601 of the source of island arc magmatism. Thus, the prograde lithologies possibly provide a

602 component, enriched in boron by at least an order of magnitude relative to primitive mantle,
603 capable of contributing to the observed boron isotope heterogeneity in ocean island basalts.
604
605 **Acknowledgements**
606
607 JH was supported in this work by the University of Leeds and a research grant from the
608 Fearnsides Fund of The Geological Society of London. CM and JAPN have been supported
609 by an EU-FP7-funded Marie Curie postdoctoral grant under contract agreement PERG08-
610 GA- 2010-276867 and PIOF-GA-2010-273017 respectively. Grants from the Ministerio de
611 Economía y Competitividad (CGL2009-12518/BTE, CGL2010-14848/BTE and CGL2012-
612 32067) and Junta de Andalucía (research groups RNM-145 and RNM-131) are also
613 acknowledged. We would also like to thank Laurie Reisberg for her editorial support and
614 Horst Marschall and an anonymous reviewer for their thought-provoking reviews.
615
616 **References**
617
618 Agranier, A., Lee, C.-T.A., Li, Z.-X.A., Leeman, W.P., 2007. Fluid-mobile element budgets
619 in serpentinized oceanic lithospheric mantle: insights from B, As, Li, Pb, PGEs and Os
620 isotopes in the Feather River Ophiolite, California. Chem. Geol. 245, 230–241.
621 doi:10.1016/j.chemgeo.2007.08.008.
622
623 Alt, J.C., Garrido, C.J., Shanks III, W.C., Turchyn, A., Padrón-Navarta, J.-A., López
624 Sánchez-Vizcaíno, V., Gómez-Pugnaire, M.T., Marchesi, C., 2012. Recycling of water,
625 carbon, and sulfur during subduction of serpentinites: A stable isotope study of Cerro

626 del Almirez, Spain. Earth Planet. Sci. Lett. 327-328, 50–60.
627 doi:10.1016/j.epsl.2012.01.029.
628
629 Amini, M., Eisenhauer, A., Böhm, F., Fietzke, J., Bach, W., Garbe-Schönberg, D., Rosner,
630 M., Bock, B., Lackschweitz, K. S., Hauff, F., 2008. Calcium isotope (δ44/40Ca)
631 fractionation along hydrothermal pathways, Logatchev field (Mid-Atlantic Ridge,
632 14°45'N). Geochim. Cosmochim. Acta 72, 4107–4122. doi:10.1016/j.gca.2008.05.055
633
634 Arculus, R.J., Powell, R., 1986. Source component mixing in the regions of arc magma
635 generation. J. Geophys. Res. B91, 5913-5926.
636
637 Bach, W., Garrido, C.J., Paulick, H., Harvey, J., Rosner, M., 2004. Seawater-peridotite
638 interactions: First insights from ODP Leg 209, MAR 15°N. Geochem. Geophys. Geosys.
639 5. doi:10.1029/2004GC000744.
640
641 Bakker, H.E., De Jong, K., Helmers, H., Biermann, C., 1989. The geodynamic evolution of
642 the Internal Zone of the Betic Cordilleras (south-east Spain): a model based on
643 structural analysis and geothermobarometry. J. Metamorphic Geol. 7, 359-381.
644
645 Baxter, E.F., Caddick, M.J., 2013. Garnet growth as a proxy for progressive subduction zone
646 dehydration. Geology 41, 643-646. http://dx.doi.org/10.1130/G34004.1
647
648 Bebout, G.E., Ryan, J.G., Leeman, W.P., 1993. B-Be systematics in subduction-related
649 metamorphic rocks: Characterization of the subducted component. Geochim.
650 Cosmochim. Acta 57, 2222-2237.

651

652 Benton, L.D., Ryan, J.G., Tera, F., 2001. Boron isotopes systematics of slab fluids as inferred
653 from a serpentine seamount, Mariana forearc. Earth Planet. Sci. Lett. 187, 273–282.
654

655 Bonatti, E., Lawrence, J.R., Morandi, N., 1984. Serpentinization of oceanic peridotites:
656 temperature dependence of mineralogy and boron content. Earth Planet. Sci. Lett. 70,
657 88–94.
658

659 Boschi, C., Dini, A., Früh-Green, G., Kelley, D.S., 2008. Isotopic and element exchange
660 during serpentinization and metasomatism at the Atlantis massif (MAR 30 N): insights
661 from B and Sr isotope data. Geochim. Cosmochim. Acta 72, 1801–1823.
662 doi:10.1016/j.gca.2008.01.013.
663

664 Bouvier, A.-S, Métrich, N., Deloule, E., 2008. Slab-derived fluids in the magma source of St.
665 Vincent (Lesser Antilles arc): Volatile and light element imprints. J. Petrol. 49 (8),
666 1427-1448. doi:10.1093/petrology/egn031.
667

668 Brenan, J.M., Ryerson, F.J., Shaw, H.F., 1998. The role of aqueous fluids in the slab-to-
669 mantle transfer of boron, beryllium, and lithium during subduction. Experiments and
670 models. Geochim. Cosmochim. Acta 62, 3337-3347.
671

672 Catanzaro E.J., Champion C.E., Garner E.L., Marienko O., Sappenfield K.M., Shields W.R.,
673 1970. Boric acid: Isotopic and assay standard reference materials. US National Bureau
674 of Standards, Special Publication 260-17, 70pp.
675

676 Chaussidon, M., Jambon, A., 1994. Boron content and isotopic composition of oceanic
677 basalts: geochemical and cosmochemical implications. Earth Planet. Sci. Lett. 121,
678 277-291.
679
680 Chaussidon, M., Marty, B., 1995. Primitive boron isotope composition of the mantle. Science
681 269, 383-386.
682
683 Deschamps, F., Guillot, S., Godard, M., Chauvel, C., Andreani, M., Hattori, K., 2010. In situ
684 characterization of serpentinites from forearc mantle wedges: Timing of
685 serpentinization and behavior of fluid-mobile elements in subduction zones. Chem.
686 Geol. 269, 262-277. doi:10.1016/j.chemgeo.2009.10.002.
687
688 Deschamps, F., Guillot, S., Godard, M., Andreani, M., Hattori, K., 2011. Serpentinites act as
689 sponges for fluid-mobile elements in abyssal and subduction zone environments. Terra
690 Nova 23, 171–178. doi: 10.1111/j.1365-3121.2011.00995.x.
691
692 Deschamps, F., Godard, M., Guillot, S., Chauvel, C., Andreani, M., Hattori, K., Wunder, B.,
693 France, L., 2012. Behaviour of fluid-mobile elements in serpentines from abyssal to
694 subduction environments: Examples from Cuba and Dominican Republic. Chem. Geol.
695 312-313, 93-117. doi:10.1016/j.chemgeo.2012.04.009.
696
697 Deschamps, F., Goddard, M., Guillot, S., Hattori, K., 2013. Geochemistry of subduction zone
698 serpentinites: A review. Lithos 178, 96-127.
699 http://dx.doi.org/10.1016/j.lithos.2013.05.019.
700

Dragovic, B., Samanta, L.M., Baxter, E.F., Selverstone, J., 2012. Using garnet to constrain the duration and rate of water-releasing metamorphic reactions during subduction: An example from Sifnos, Greece. Chem. Geol. 314-317, 9–22. doi:10.1016/j.chemgeo.2012.04.016.

Evans, B.W., Johannes, W., Oterdoom, H., Trommsdorff, V., 1976. Stability of chrysotile and antigorite in the serpentinite multisystem: Schweizer Mineralogische und Petrographische Mitteilungen 56, 79–93.

Faccenda, M., Gerya, T.V., Burlini, L., 2009. Deep slab hydration induced by bending-related variations in tectonic pressure. Nature Geosci. 2, 790-793. doi: 10.1038/NGEO656.

Foster, G.L., Pogge von Strandmann, P.A.E., Rae, J.W.B., 2010. Boron andmagnesium isotopic composition of seawater. Geochem. Geophys. Geosys. 11(8): Q08015, doi:10.1029/2010GC003201.

Foustoukos, D.I., Savov, I.P., Janecky, D.R., 2008. Chemical and isotopic constraints on water/rock interactions at the Lost City hydrothermal field, 30° N Mid-Atlantic Ridge. Geochim. Cosmochim. Acta 72, 5457-5474. doi:10.1016/j.gca.2008.07.035.

Fryer, P., 2011. Serpentinite Mud Volcanism: Observations, Processes, and Implications. Ann. Rev. Earth Planet. Sci. 4.19, 1-29. doi:10.1146/annurev-marine-120710-100922.

725 Fryer, P., Gharib, J., Ross, K., Savov, I., Mottl, M.J., 2006. Variability in serpentinite
726 mudflow mechanisms and sources: ODP drilling results on Mariana forearc seamounts.
727 Geochem. Geophys. Geosys. 7 (8), Q08014. doi:10.1029/2005GC001201.
728
729 Fryer, P., Ambos, E.L., Hussong, D.M., 1985. Origin and emplacement of Mariana Forearc
730 seamounts. Geology 13, 774–777.
731
732 Garrido, C.J., López Sánchez-Vizcaíno, V., Gómez-Pugnaire, M.T., Trommsdorff, V., Alard,
733 O., Godard, M., 2005. Enrichment of HFSE in chlorite–harzburgite produced by high-
734 pressure dehydration of antigorite–serpentinite; implications for subduction
735 magmatism. Geochem. Geophys. Geosys. 6 (1). doi:10.1029/ 2004GC000791.
736
737 Gerya, T.V., Yuen, D.A., 2003. Rayleigh-Taylor instabilities from hydration and melting
738 propel 'cold plumes' at subduction zones. Earth Planet. Sci. Lett. 212, 47-62.
739
740 Gerya, T.V., Stoeckhert, B., Perchuk, A.L., 2002. Exhumation of high-pressure metamorphic
741 rocks in a subduction channel; a numerical simulation. Tectonics 21, 6-19.
742
743 Gómez-Pugnaire, M.T., Franz, G., 1988. Metamorphic evolution of the Palaeozoic series of
744 the Betic Cordillera (Nevado-Filábride complex, SE Spain) and its relationship with the
745 Alpine orogeny. Geologische Rundschau 77, 619-640.
746
747 Hacker, B.R., Peacock, S.M., Abers, G.A., Holloway, S.D., 2003. Subduction factory 2. Are
748 intermediate-depth earthquakes in subducting slabs linked to metamorphic dehydration

749 reactions? J. Geophys Res - Solid Earth 108 (B1) 2030. doi:10.1029/2001JB001129,
750 2003.
751
752 Harvey, J., Savov, I.P., Agostini, S., Cliff, R.A., Walshaw, R.D., 2014. Si-metasomatism in
753 serpentinized peridotite: the effects of talc-alteration on strontium and boron isotopes in
754 abyssal peridotites from Hole 1268a, ODP Leg 209. Geochim. Cosmochim. Acta 126,
755 30-48. http://dx.doi.org/10.1016/j.gca.2013.10.035.
756
757 Hattori, K., Guillot, S., 2003. Volcanic fronts form as a consequence of serpentinite
758 dehydration in the forearc mantle wedge. Geology 31(6), 525-528.
759
760 Hattori, K., Guillot, S., 2007. Geochemical character of serpentinites associated with high- to
761 ultrahigh-pressure metamorphic rocks in the Alps, Cuba, and the Himalayas: Recycling
762 of elements in subduction zones. Geochem. Geophys. Geosys. 8 (9) Q09010.
763 doi:10.1029/2007GC001594.
764
765 Hürlimann, R., 1999. Die Hochdruckmetamorphose der Ultramafika und der angrenzenden
766 Nebengesteine am Cerro de Almirez Sierra Nevada, Südspanien: Teil II. Diplomarbeit,
767 ETH, Zürich, 105 p.
768
769 Hyndman, R.D., Peacock, S.M., 2003. Serpentinization of the forearc mantle. Earth Planet.
770 Sci. Lett. 212, 417-432. doi:10.1016/S0012-821X(03)00263-2.
771
772 Ishikawa, T., Nakamura, E., 1993. Boron isotope systematics of marine sediments. Earth
773 Planet. Sci. Lett. 117, 567-580.

774

775 Ishikawa, T., Nakamura, E., 1994. Origin of the slab component in arc lavas from across-arc
776 variation of B and Pb isotopes. Nature 370, 205–208.

777

778 Ishikawa, T., Tera, F., 1997. Source, composition and distribution of the fluid in Kurile
779 mantle wedge: Constraints from across-arc variations of B/Nb and B isotopes. Earth
780 Planet. Sci. Lett. 152, 123–138.

781

782 Ishikawa, T., Tera, F., 1999. Two isotopically distinct fluid components involved in the
783 Mariana arc: Evidence from Nb/B ratios and B, Sr, Nd. and Pb isotope systematics.
784 Geology 27, 83–86.

785

786 Ishikawa, T., Tera, F., Nakazawa, T., 2001. Boron isotope and trace element systematics of
787 the three volcanic zones in the Kamchatka arc. Geochim. Cosmochim. Acta 65 (24),
788 4523-4537.

789

790 Janecky, D.R., Seyfried Jr., W.E., 1986. Hydrothermal serpentinization of peridotite within
791 the oceanic crust: experimental investigations of mineralogy and major element
792 chemistry. Geochim. Cosmochim. Acta 50, 1357−1378.

793

794 John, T., Gussone, N., Podladchikov, Y.Y., Bebout, G.E., Dohmen, R., Halama, R., Klemd,
795 R., Magna, T., Seitz, H.-M., 2012. Volcanic arcs fed by rapid pulsed flow through
796 subducting slabs. Nature Geosci. 5, 489-492. doi: 10.1038/ngeo1482.

797

798 Kendrick, M.A., Scambelluri, M., Honda, M., Phillips, D., 2011. High abundances of noble
799 gas and chlorine delivered to the mantle by serpentinite subduction. Nature Geosci. 4,
800 807-812. doi: 10.1038/ngeo1270.
801
802 Kendrick, M.A., Woodhead, J.D., Kamenetsky, V., 2012. Tracking halogens through the
803 subduction cycle. Geology 40 (12), 1075-1078. doi:10.1130/G33265.1.
804
805 Kerrick, D.M., Connolly, J.A.D., 2001. Metamorphic devolatilization of subducted oceanic
806 metabasalts: implications for seismicity, arc magmatism and volatile recycling. Earth
807 Planet. Sci. Lett. 189, 19–29.
808
809 King, R.L., Kohn, M.J., Eiler, J.M., 2003. Constraints on the petrologic structure of the
810 subduction zone slab-mantle interface from Franciscan Complex exotic ultramafic
811 blocks. Geol. Soc. Am. Bull. 115, 1097-1109.
812
813 Kodolányi, J., Pettke, T., 2011. Loss of trace elements from serpentinites during fluid-
814 assisted transformation of chrysotile to antigorite - An example from Guatemala. Chem.
815 Geol. 284, 351-362. doi:10.1016/j.chemgeo.2011.03.016.
816
817 Komor, S.C., Elthon, D., Casey, J.F., 1985. Serpentinization of cumulate ultramafic rocks
818 from the North Arm Mountain massif of the Bay of Islands ophiolite. Geochim.
819 Cosmochim. Acta 49, 2331−2338.
820

821 Leeman, W.P., Tonarini, S., Chan, L.H., Borg, L.E., 2004. Boron and lithium isotopic
822 variations in a hot subduction zone - The southern Washington Cascades. Chem. Geol.
823 212, 101–124. doi:10.1016/j.chemgeo.2004.08.010.
824
825 Lehnert, K., Su, Y., Langmuir, C., Sarbas, B., Nohl, U., 2000. A global geochemical database
826 structure for rocks. Geochem. Geophys. Geosys. 1. doi:10.1029/1999GC000026.
827
828 López Sánchez-Vizcaíno, V., Rubatto, D., Gómez-Pugnaire, M.T., Trommsdorff, V.,
829 Müntener, O., 2001. Middle Miocene high-pressure metamorphism and fast
830 exhumation of the Nevado-Filabride Complex, SE Spain. Terra Nova 13, 327-332.
831
832 Marchesi, C., Garrido, C.J., Padrón-Navarta, J. A., López Sánchez-Vizcaíno, V., Gómez-
833 Pugnaire, M.T., 2013. Element mobility from seafloor serpentinization to high-
834 pressure dehydration of antigorite in subducted serpentinite: insights from the Cerro
835 del Almirez ultramafic massif (southern Spain). Lithos 178, 128-142. doi:
836 10.1016/j.lithos.2012.11.025.
837
838 Marschall, H.R., Ludwig, T., Altherr, R., Kalt, A., Tonarini, S., 2006. Syros metasomatic
839 tourmaline: Evidence for very high $\delta^{11}B$ fluids in subduction zones: J. Petrol. 47, 1915–
840 1942. doi:10.1093/petrology/egl031.
841
842 Marschall, H.R., Schumacher, J.C., 2012. Arc magmas sourced from mélange diapirs in
843 subduction zones. Nature Geosci. 5, 862-867. doi: 10.1038/ngeo1634.
844

Miyashiro, A., Shido, F., Ewing, M., 1969. Composition and origin of serpentinites from the Mid-Atlantic Ridge near 24° and 30° north latitude. Contrib. Mineral. Petrol. 23, 117–127.

Morris, J.D., Ryan, J.G., 2003. Subduction zone processes and implications for changing composition of the upper and lower mantle. In: The Mantle and Core, v. 2, Treatise on Geochemistry, edited by H. D. Holland and K. K. Turekian, pp. 451–471, Elsevier, New York.

Morten, L., Puga, E., 1984. Blades of olivines and orthopyroxenes in ultramafic rocks from the Cerro del Almirez, Sierra Nevada Complex, Spain: relics of quench-textured harzburgites? Neues Jahrbuch für Mineralogie, Monatshefte 211-218.

Mottl, M.J., 1992. Pore waters from serpentinite seamounts in the Mariana and Izu-Bonin forearcs, Leg 125: Evidence for volatiles from the subducting slab. Proc. ODP, Scientific Results 125, 373–387.

O'Hanley, D.S., 1996. Serpentinite records of tectonic and petrological history. Oxford Monographs on Geology and Geophysics, vol. 34. Oxford University Press. 277 pp.

Pabst, S., Zack, T., Savov, I.P., Ludwig, T., Rost, D., Vicenzi, E.P., 2011. Evidence for boron incorporation into the serpentine crystal structure. American Mineralogist 96, 1112–1119.

869 Pabst, S., Zack, T., Savov, I.P., Ludwig, T., Rost, D., Tonarini, S., Vicenzi, E.P., 2012. The
870 fate of subducted oceanic slabs in the shallow mantle: Insights from boron isotopes and
871 light element composition of metasomatized blueschists from the Mariana forearc.
872 Lithos 132-133, 162-179. doi:10.1016/j.lithos.2011.11.010.
873
874 Padrón-Navarta, J. A., Hermann, J., Garrido, C.J., López Sánchez-Vizcaíno, V., Gómez-
875 Pugnaire, M.T., 2010. An experimental investigation of antigorite dehydration in
876 natural silica-enriched serpentinite. Contrib. Mineral. Petrol. 159, 25-42. doi
877 10.1007/s00410-009-0414-5.
878
879 Padrón-Navarta, J. A., López Sánchez-Vizcaíno, V., Garrido, C.J., Gómez-Pugnaire, M.T.,
880 2011. Metamorphic Record of High-pressure Dehydration of Antigorite Serpentinite to
881 Chlorite Harzburgite in a Subduction Setting (Cerro del Almirez, Nevado-Filábride
882 Complex, Southern Spain). J. Petrol. 52 (10), 2047-2078.
883 doi:10.1093/petrology/egr039.
884
885 Palmer, M.R., 1991. Boron-isotope systematics of Halmahera arc (Indonesia) lavas: Evidence
886 for involvement of the subducted slab. Geology 19, 217-217.
887
888 Palmer, M.R., Edmond, J., 1989. The strontium isotope budget of the modern ocean. Earth
889 Planet. Sci. Lett. 92, 11–26.
890
891 Paulick, H., Bach, W., Godard, M., Hoog, C.-J., Suhr, G., Harvey, J., 2006. Geochemistry of
892 abyssal peridotites (Mid-Atlantic Ridge, 15°20′N, ODP Leg 209): implications for
893 fluid/rock interaction in slow spreading environments. Chem. Geol. 234, 179–210.

894

895 Peacock, S.M., Hervig, R.L., 1999. Boron isotopic composition of subduction-zone
896 metamorphic rocks. Chem. Geol. 160, 281–290. doi:10.1016/S0009-2541(99)00103-5.
897

898 Pearce, J.A., Parkinson, I.J., 1993. Trace element models for mantle melting: application to
899 volcanic arc petrogenesis. In: Prichard, H.M., Alabaster, T., Harris, N.B.W. & Neary,
900 C.R. (eds), 1993, Magmatic Processes and Plate Tectonics, Geol. Soc. Spec. Pub. 76,
901 373-403.
902

903 Puga, E., Nieto, J.M., Díaz de Federico, A., Bodinier, J.-L., Morten, L., 1999. Petrology and
904 metamorphic evolution of ultramafic rocks and dolerite dykes of the Betic Ophiolitic
905 Association (Mulhacen Complex, SE Spain): evidence of eo-Alpine subduction
906 following an ocean-floor metasomatic process. Lithos 49, 23-56.
907

908 Ranero, C.R., Morgan, J.P., Reichert, C., 2003. Bending-related faulting and mantle
909 serpentinization at the Middle America trench. Nature 425, 367-373.
910

911 Ranero, C.R., Sallares., V., 2004. Geophysical evidence for hydration of the crust and mantle
912 of the Nazca plate during bending at the north Chile trench. Geology 32 (7), 549-552.
913 doi: 10.1130/G20379.1.
914

915 Ribeiro da Costa, I., Barriga, F.J.A. S., Viti, C., Mellini, M., Wicks, F.J., 2008. Antigorite in
916 deformed serpentinites from the Mid-Atlantic Ridge. Eur. J. Mineral. 20, 563–572.
917

Ryan, J.G., Langmuir, C.H., 1993. The systematics of boron abundances in young volcanic rocks. Geochim. Cosmochim. Acta 57, 1489–1498.

Salters, V.J.M., Stracke, A., 2004. Composition of the depleted mantle: Geochem. Geophys. Geosys. 5, Q05B07. doi:10.1029/2003GC000597.

Savov, I.P., Ryan, J.G., D'Antonio, M., Kelley, K., Mattie, P., 2005. Geochemistry of serpentinized peridotites from the Mariana Forearc Conical Seamount, ODP Leg 125: Implications for the elemental recycling at subduction zones. Geochem. Geophys. Geosys. 6, Q04J15. doi:10.1029/2004GC000777.

Savov, I.P., Ryan, J.G., D'Antonio, M., Fryer, P., 2007. Shallow slab fluid release across and along the Mariana arc-basin system: Insights from geochemistry of serpentinized peridotites from the Mariana Forearc. J. Geophys. Res. 112, B09205. doi:10.1029/2006JB004749.

Scambelluri, M., Müntener, O., Hermann, J., Piccardo, G.B., Trommsdorff, V., 1995. Subduction of water into the mantle: History of an Alpine peridotite. Geology 25, 459-462.

Scambelluri, M., Müntener, O., Ottolini, L., Pettke, T., Vannucci, R., 2004. The fate of B, Cl and Li in the subducted oceanic mantle and in the antigorite breakdown fluids. Earth Planet. Sci. Lett. 222, 217–234.

942 Scambelluri, M., Tonarini, S., 2012. Boron isotope evidence for shallow fluid transfer across
943 subduction zones by serpentinized mantle. Geology 40, 907–910.
944 doi:10.1130/G33233.1.
945
946 Schmidt, M.W., Poli, S., 1998. Experimentally based water budgets for dehydrating slabs and
947 consequences for arc magma generation. Earth Planet. Sci. Lett. 163, 361-379.
948
949 Schönbächler, M., 1999. Die Hochdruckmetamorphose der Ultramafika und der
950 angrenzenden Nebengesteine am Cerro de Almirez-Sierra Nevada, Südspanien:
951 Diplomarbeit, ETH Zürich, 113 p.
952
953 Schwartz, S., Guillot, S., Reynard, B., Lafay, R., Debret, B., Nicollet, C., Lanari, P.,
954 Auzende, A.L., 2013. Pressure–temperature estimates of the lizardite/antigorite
955 transition in high pressure serpentinites. Lithos 179, 197-210
956 http://dx.doi.org/10.1016/j.lithos.2012.11.023.
957
958 Seyfried, W.E., Dibble, W.E.J., 1980. Sea water - peridotite interaction at 300 deg C and 500
959 bars: Implications for the origin of oceanic serpentinites. Geochim. Cosmochim. Acta
960 44, 309–321.
961
962 Seyfried, W.E., Janecky, D.R., Mottl, M.J., 1984. Alteration of the oceanic crust:
963 Implications for geochemical cycles of lithium and boron. Geochim. Cosmochim. Acta
964 44, 557-569.
965

966 Smith, H.J., Spivack, A.J., Hart, S.R., 1995. The boron isotopic composition of altered
967 oceanic crust. Chem. Geol. 126, 119-135.
968
969 Spandler, C., Hermann, J., Faure, K., Mavrogenes, J. A., Arculus, R., 2008. The importance
970 of talc and chlorite hybrid rocks for volatile recycling through subduction zones;
971 evidence from the high-pressure subduction mélange of New Caledonia. Contrib.
972 Mineral. Petrol. 155, 181-198. doi 10.1007/s00410-007-0236-2.
973
974 Straub, S.M., Layne, G.D., 2003. The systematics of chlorine, fluorine, and water in Izu arc
975 front volcanic rocks: Implications for volatile recycling in subduction zones. Geochim.
976 Cosmochim. Acta 67, 4179–4203.
977
978 Sumino, H., Burgess, R., Mizukami, T., Wallis, S.R., Holland, G., Ballentine, C.J., 2010.
979 Seawater-derived noble gases and halogens preserved in exhumed mantle wedge
980 peridotite. Earth Planet. Sci. Lett. 294, 163-172. doi:10.1016/j.epsl.2010.03.029.
981
982 Tenthorey, E., Hermann, J., 2004. Composition of fluids during serpentinite breakdown in
983 subduction zones: Evidence for limited boron mobility. Geology 32 (10), 865-868.
984 doi:10.1130/G20610.1.
985
986 Thompson, G., Melson, W.G., 1970. Boron contents of serpentinites and metabasalts in the
987 oceanic crust: Implications for the boron cycle in the oceans. Earth Planet. Sci. Lett. 8,
988 61–65.
989

990 Tonarini, S., Pennisi, M., Leeman, W.P., 1997. Precise boron analysis of complex silicate
991 (rock) samples using alkali carbonate fusion and ion exchange separation. Chem. Geol.
992 142, 129–137.
993
994 Tonarini, S., Armienti. P., D'Orazio, M., Innocenti, F., 2001. Subduction-like fluids in the
995 genesis of Mt. Etna magmas: evidence from boron isotopes and fluid mobile elements.
996 Earth Planet. Sci. Lett. 192, 471-483.
997
998 Tonarini, S., Pennisi, M., Adorni-Braccesi, A., Dini, A., Ferrara, G., Gonfiantini, R.,
999 Wiedenbeck, M., Gröning, M., 2003. Intercomparison of boron isotope and
1000 concentration measurements: Part I: Selection, preparation and homogeneity tests of the
1001 intercomparison materials. Geostandards Newsletter 27, 21–39.
1002
1003 Tonarini, S., Agostini, S., Doglioni, C., Innocenti, F., Manetti, P., 2007. Evidence for
1004 serpentinite fluid in convergent margin systems: The example of El Salvador (Central
1005 America) arc lavas. Geochem. Geophys. Geosys. 8 (9), Q09014.
1006 doi:10.1029/2006GC001508.
1007
1008 Tonarini, S., Leeman, W.P., Leat, P.T., 2011. Subduction erosion of forearc mantle wedge
1009 implicated in the genesis of the South Sandwich Island (SSI) arc: Evidence from boron
1010 isotope systematics. Earth Planet. Sci. Lett. 301, 275-284.
1011 doi:10.1016/j.epsl.2010.11.008.
1012

1013 Trommsdorff, V., López Sánchez-Vizcaíno, V., Gómez-Pugnaire, M.T., Müntener, O., 1998.
1014 High pressure breakdown of antigorite to spinifex-textured olivine and orthopyroxene,
1015 SE Spain. Contrib. Mineral. Petrol. 132, 139-148.
1016
1017 Ukar, E. 2012. Tectonic significance of low-temperature blueschist blocks in the Franciscan
1018 mélange at San Simeon, California. Tectonophys. 568-569, 154-169.
1019 doi:10.1016/j.tecto.2011.12.039.
1020
1021 Ukar, E., Cloos, M., Vasconcelos, P., 2012. First ^{40}Ar-^{39}Ar Ages from Low-T Mafic
1022 Blueschist Blocks in a Franciscan Mélange near San Simeon: Implications for Initiation
1023 of Subduction. J. Geol. 120, 543-556. doi: 10.1086/666745.
1024
1025 Vils, F., Pelletier, L., Kalt, A., Müntener, O., Ludwig, T., 2008. The lithium, boron and
1026 beryllium content of serpentinized peridotites from ODP Leg 209 (Sites 1272A and
1027 1274A): implications for lithium and boron budgets of oceanic lithosphere. Geochim.
1028 Cosmochim. Acta 72, 5475–5504. doi:10.1016/j.gca.2008.08.005.
1029
1030 Vils, F., Tonarini, S., Seitz, H.-M., Kalt, A., 2009. Boron, lithium and strontium isotopes as
1031 tracers of seawater–serpentinite interaction at mid-Atlantic ridge, ODP Leg 209. Earth
1032 Planet. Sci. Lett. 286, 414–425. doi:10.1016/j.epsl.2009.07.005.
1033
1034 Vils, F., Müntener, O., Kalt, A., Ludwig, T., 2011. Implications of the serpentine phase
1035 transition on the behaviour of beryllium and lithium–boron of subducted ultramafic
1036 rocks. Geochim. Cosmochim. Acta 75, 1249–1271. doi:10.1016/j.gca.2010.12.007.
1037

Wicks, F.J., Whittaker, E.J.W., 1977. Serpentine textures and serpentinization. Canadian Mineralogist 15, 459−488.

You, C.-F., Chan, L.H., Spivack, A.J., and Gieskes, J.M., 1995. Lithium, boron, and their isotopes in sediments and pore waters of Ocean Drilling Program Site 808, Nankai Trough: implications for fluid expulsion in accretionary prisms. Geology 23, 37-40.

Figure captions

Figure 1. (a) Simplified geological map showing the main tectono-metamorphic domains of the Betic Cordillera. (b) Main tectonic and lithological units of the Nevado–Filábride Complex and location of the Cerro del Almirez (inset) together with other smaller ultramafic bodies cropping out in this complex. (c) Geological map of the Cerro del Almirez (modified from Padrón-Navarta et al., 2011).

Figure 2. Field relationships between antigorite-serpentinite, transitional lithologies, and chlorite-harzburgite, and their modal variations (modified after Padrón-Navarta et al., 2011). Boron and strontium abundances ([B]) expressed in μg g^{-1}. $\delta^{11}B = \{[(^{11}B/^{10}B_{sample}) / (^{11}B/^{10}B_{NIST\text{-}SRM951}) -1] * 1000\}$. Loss on ignition (LOI) expressed in weight % H_2O.

Figure 3. Mean fluid-mobile and high field-strength element abundances in Cerro del Almirez antigorite-serpentinite (data from Marchesi et al., 2013 with the exception of boron abundances) normalized to mean abyssal serpentinite and mean mantle wedge serpentinite (Deschamps et al., 2013).

Figure 4. Relative major element abundances in prograde lithologies from Cerro del Almirez, normalized to Cerro del Almirez antigorite-serpentinite (major element abundances from Marchesi et al., 2013).

Figure 5. Relative mean trace element abundances in prograde lithologies from Cerro del Almirez, normalized to Cerro del Almirez antigorite-serpentinite (trace element abundances from Marchesi et al., 2013).

Figure 6. $\delta^{11}B$ versus Nb/B for Cerro del Amirez lithologies (unless stated symbols are the same as previous Figures). Elevated Nb/B at Cerro del Almirez are comparable to the ratios seen in arc lavas in general (diagonal shaded field). The antigorite-serpentinite however (white square) appears to have $\delta^{11}B$ and Nb/B that closely resembles the values obtained for arc magmas of the South Sandwich Arc (dotted field; Tonarini et al., 2011). Redrawn after Scambelluri et al. (2012).

Figure 7. (a) Boron isotope ratios and (b) boron elemental abundances of Cerro del Almirez serpentinites and harzburgites compared to common mafic / ultramafic lithologies and their constituent minerals (Literature values from Palmer, 1991; Ishikawa and Nakamura, 1994; Ishikawa and Tera, 1997, 1999; Benton et al., 2001; Ishikawa et al 2001; Tonarini et al., 2001, 2007, 2011; Leeman et al., 2004; Scambelluri et al., 2004 (which includes representative prograde lithologies from Cerro del Almirez); Agranier et al., 2007; Vils et al., 2008, 2009; Boschi et al., 2008; Deschamps et al., 2010, 2012; Pabst et al., 2011; Scambelluri and Tonarini, 2012).

Figure

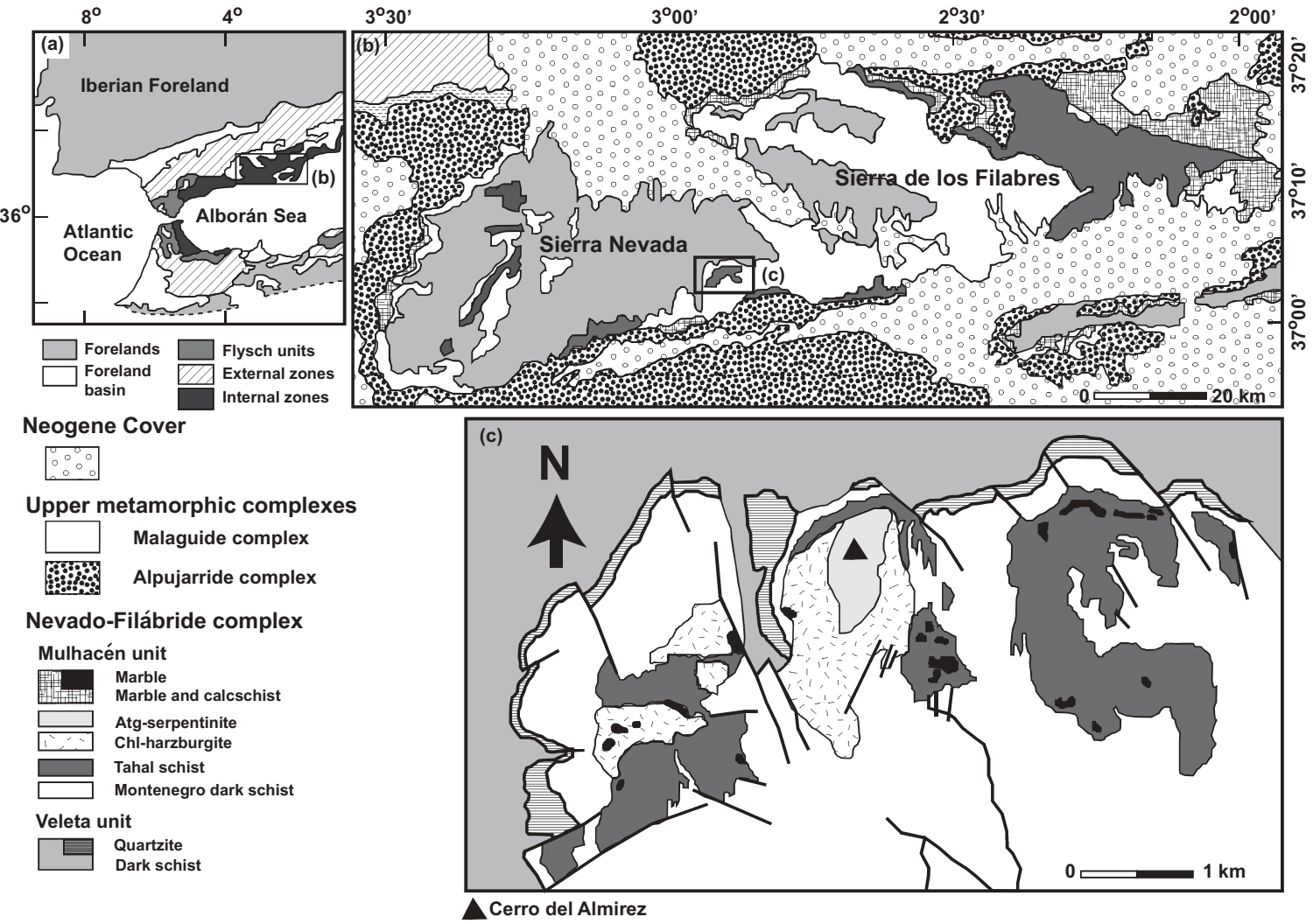
8°
4°
36°
(a)
Iberian Foreland
(b)
Alborán Sea
Atlantic Ocean
3°30'
3°00'
2°30'
2°00'
37°20'
37°10'
37°00'
Sierra de los Filabres
Sierra Nevada
(c)
0
20 km
Forelands
Foreland basin
Flysch units
External zones
Internal zones
Neogene Cover
Upper metamorphic complexes
Malaguide complex
Alpujarride complex
Nevado-Filábride complex
Mulhacén unit
Marble
Marble and calcschist
Atg-serpentinite
Chl-harzburgite
Tahal schist
Montenegro dark schist
Veleta unit
Quartzite
Dark schist
N
0
1 km
Cerro del Almirez

Figure

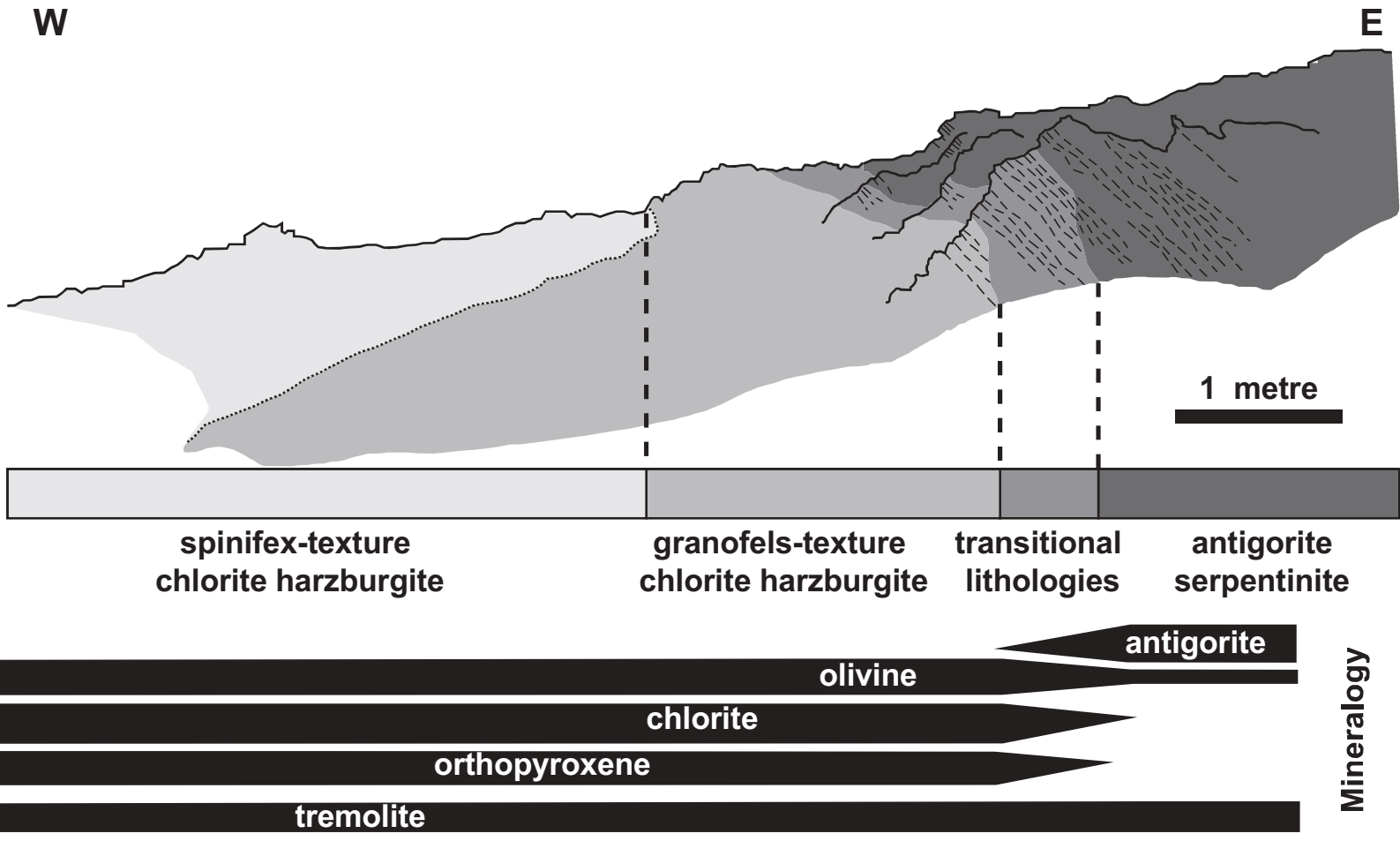

[B]	7.59 to 10.34	7.15	11.78	7.03
$\delta^{11}B$	+2.68 +/- 0.35 to +6.22 +/- 0.76	-3.3 +/- 0.27	+3.38 +/- 0.35	+22.37 +/- 0.86
LOI (wt. %)	5.44	5.94	9.62	10.14
$^{87}Sr/^{86}Sr$	0.70752 +/- 1 to 0.70763 +/- 1	0.70824 +/- 4	0.70847 +/- 3	0.70819 +/- 1 to 0.70871 +/- 2
[Sr]	5.66 to 9.50	1.23	4.33	0.33 to 2.29

Figure

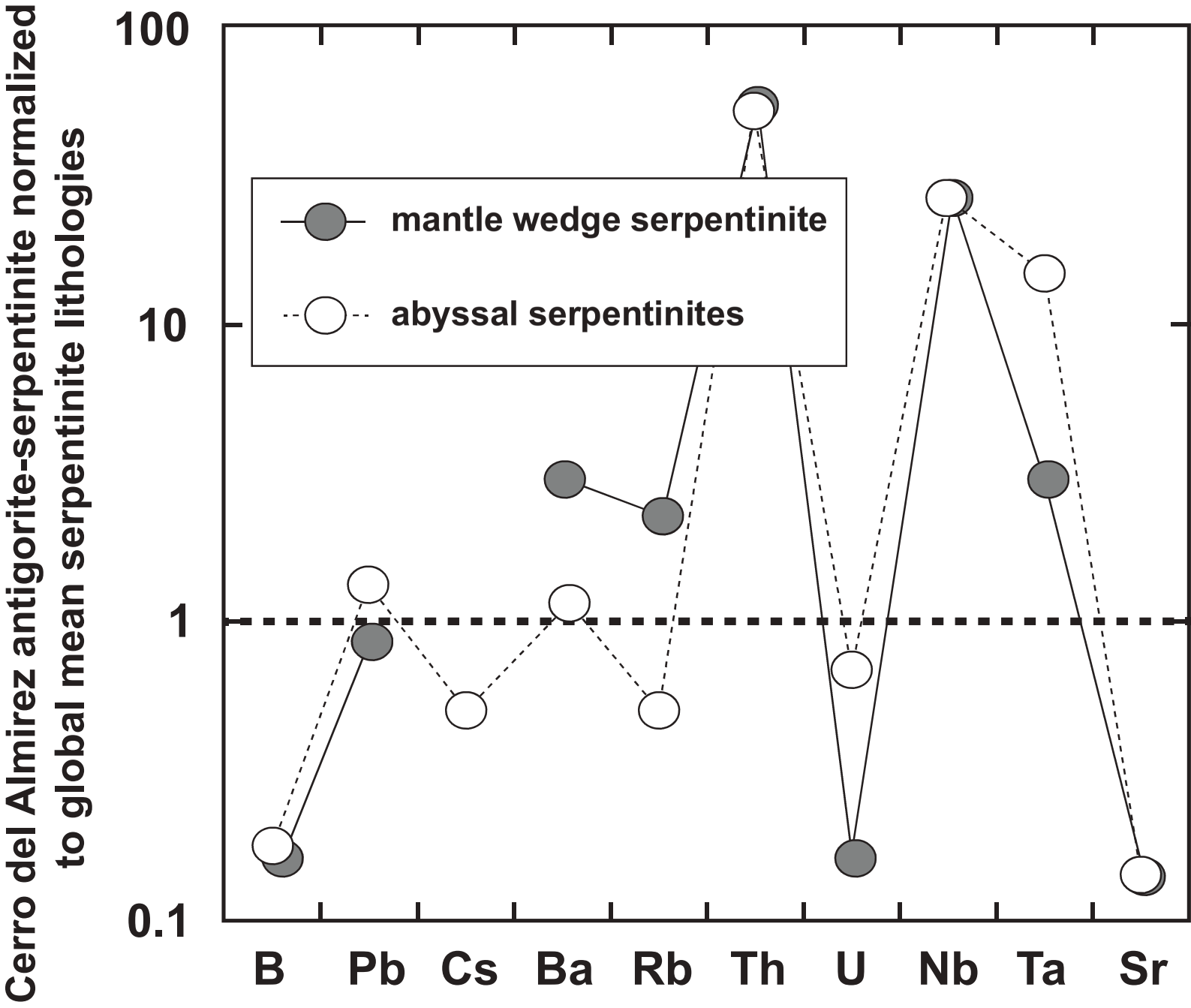
Cerro del Almirez antigorite-serpentinite normalized
to global mean serpentinite lithologies
100
10
1
0.1
mantle wedge serpentinite
abyssal serpentinites
B
Pb
Cs
Ba
Rb
Th
U
Nb
Ta
Sr

Figure

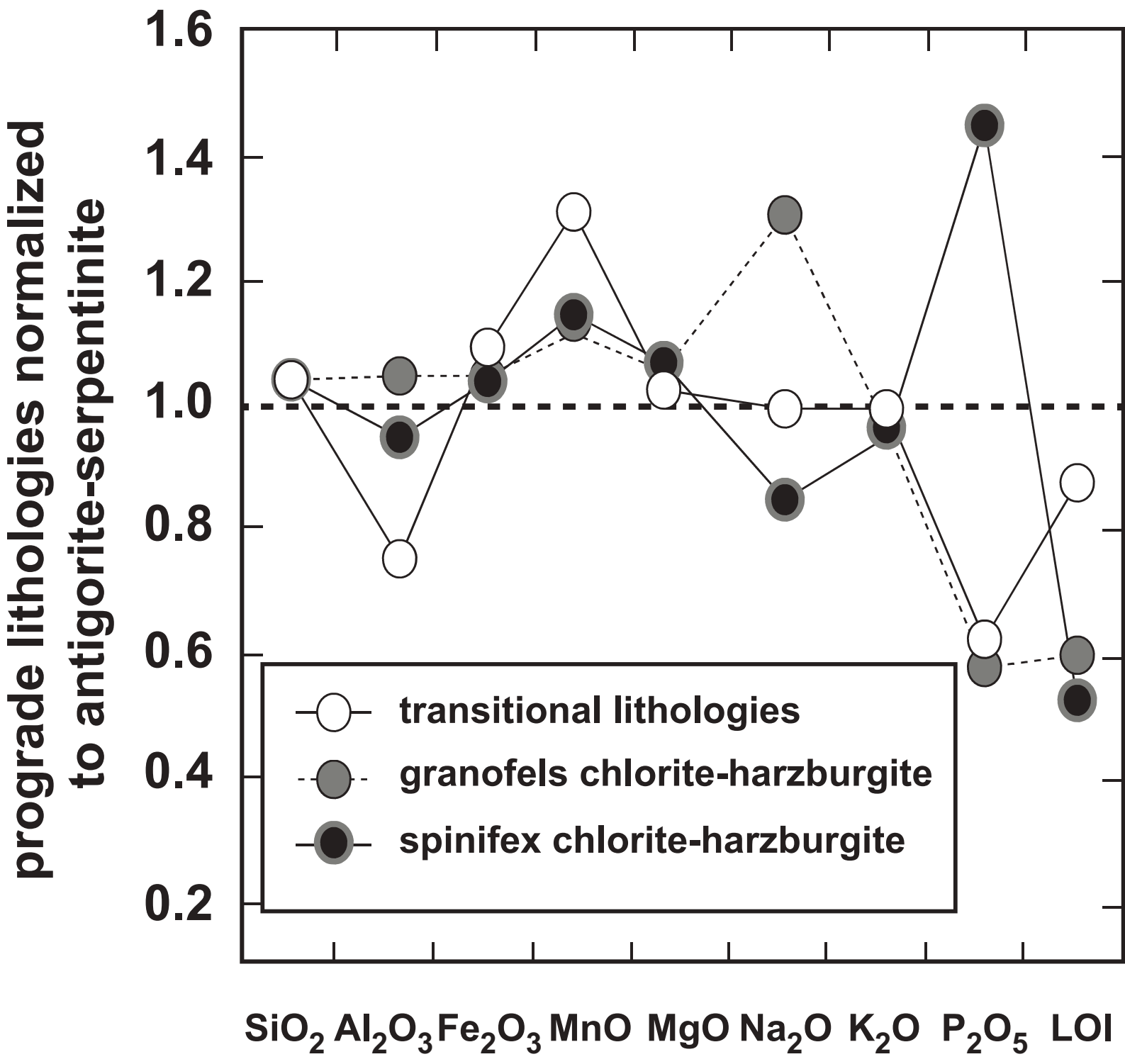
prograde lithologies normalized
to antigorite-serpentinite
1.6
1.4
1.2
1.0
0.8
0.6
0.4
0.2
transitional lithologies
granofels chlorite-harzburgite
spinifex chlorite-harzburgite
SiO2 Al2O3 Fe2O3 MnO MgO Na2O K2O P2O5 LOI

Figure

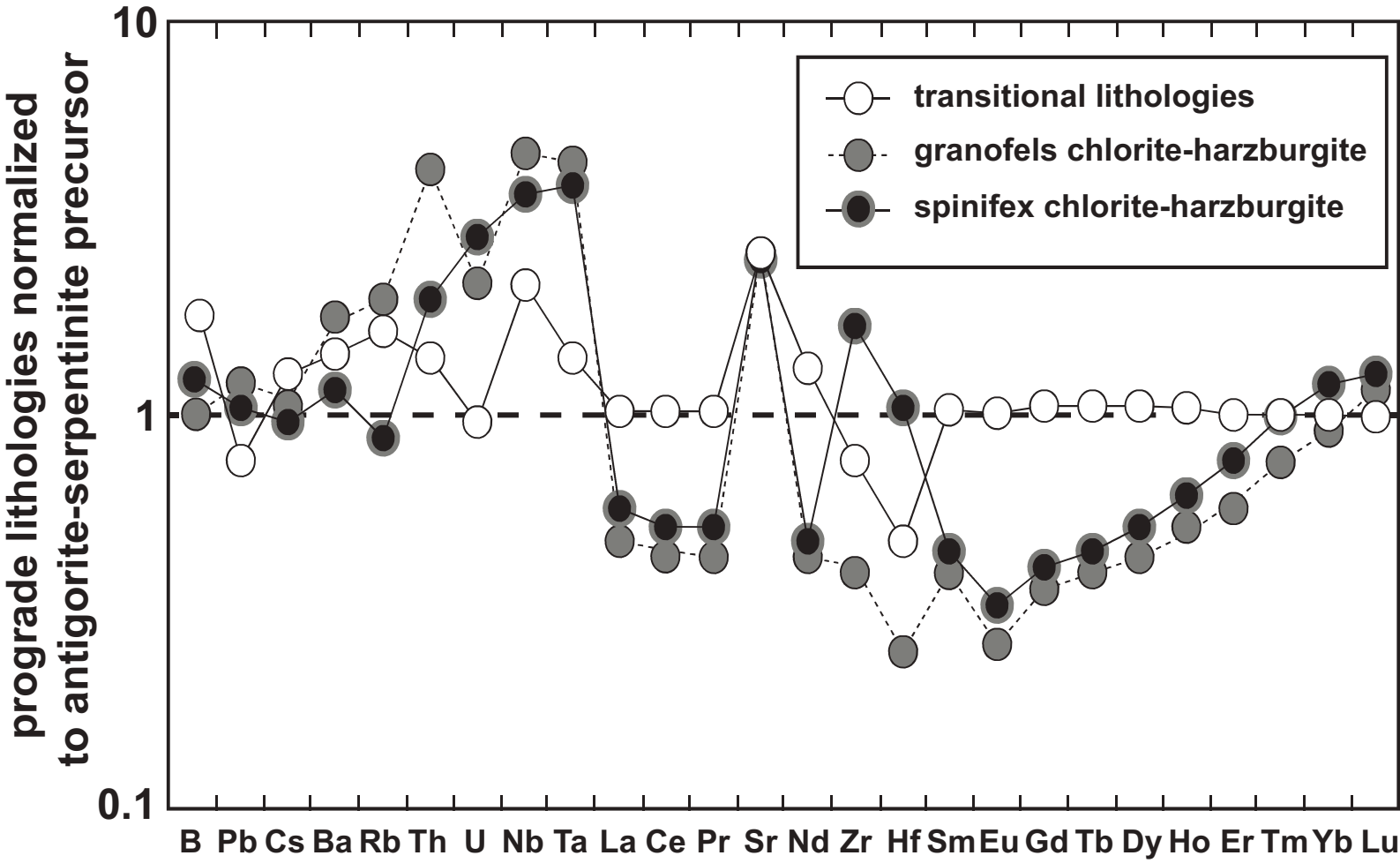
10
1
0.1
prograde lithologies normalized
to antigorite-serpentinite precursor
transitional lithologies
granofels chlorite-harzburgite
spinifex chlorite-harzburgite
B Pb Cs Ba Rb Th U Nb Ta La Ce Pr Sr Nd Zr Hf Sm Eu Gd Tb Dy Ho Er Tm Yb Lu

Figure

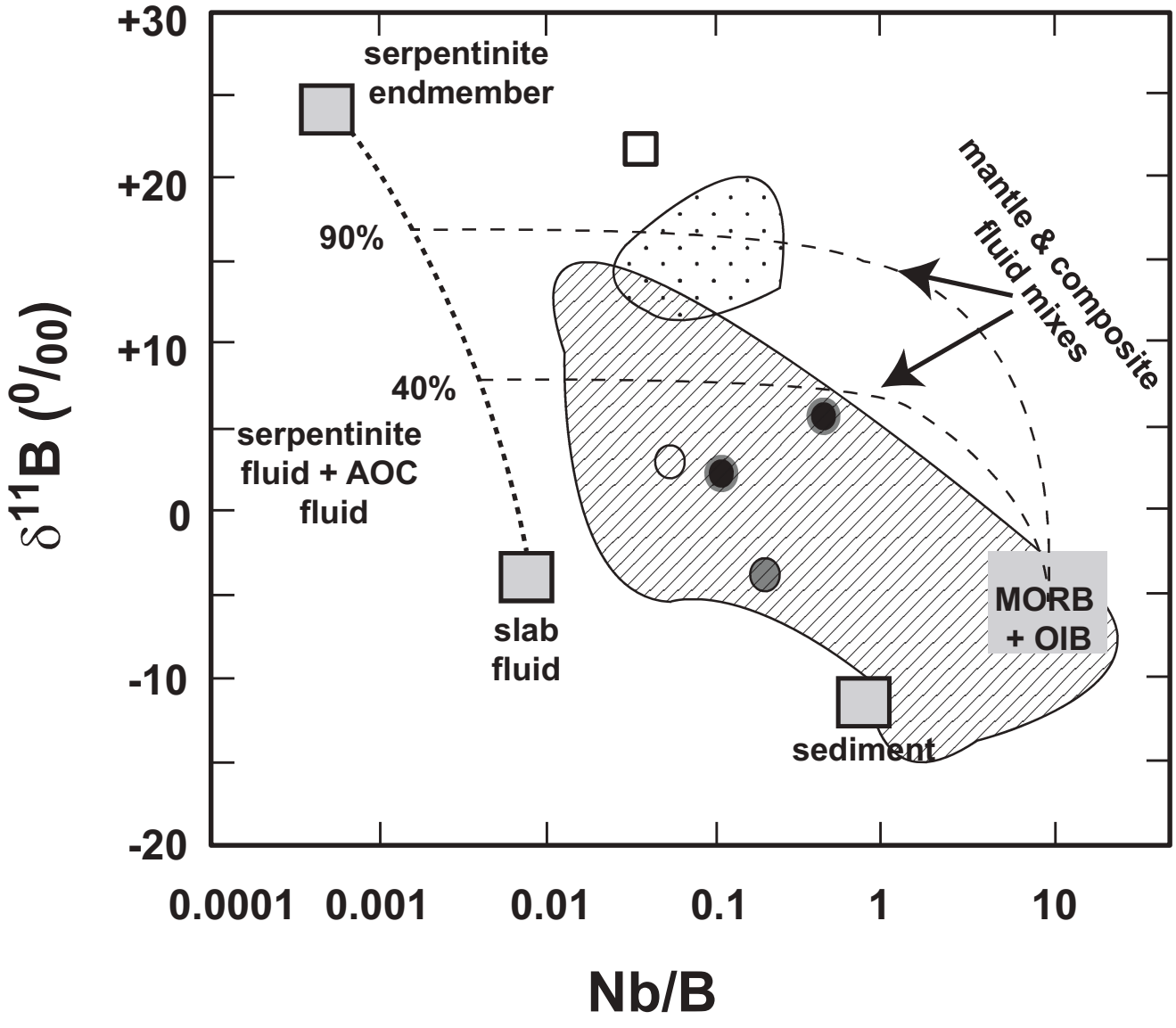
+30
+20
+10
0
-10
-20
δ11B (0/00)
0.0001
0.001
0.01
0.1
1
10
Nb/B
serpentinite endmember
90%
40%
serpentinite fluid + AOC fluid
slab fluid
mantle & composite fluid mixes
MORB + OIB
sediment

Figure

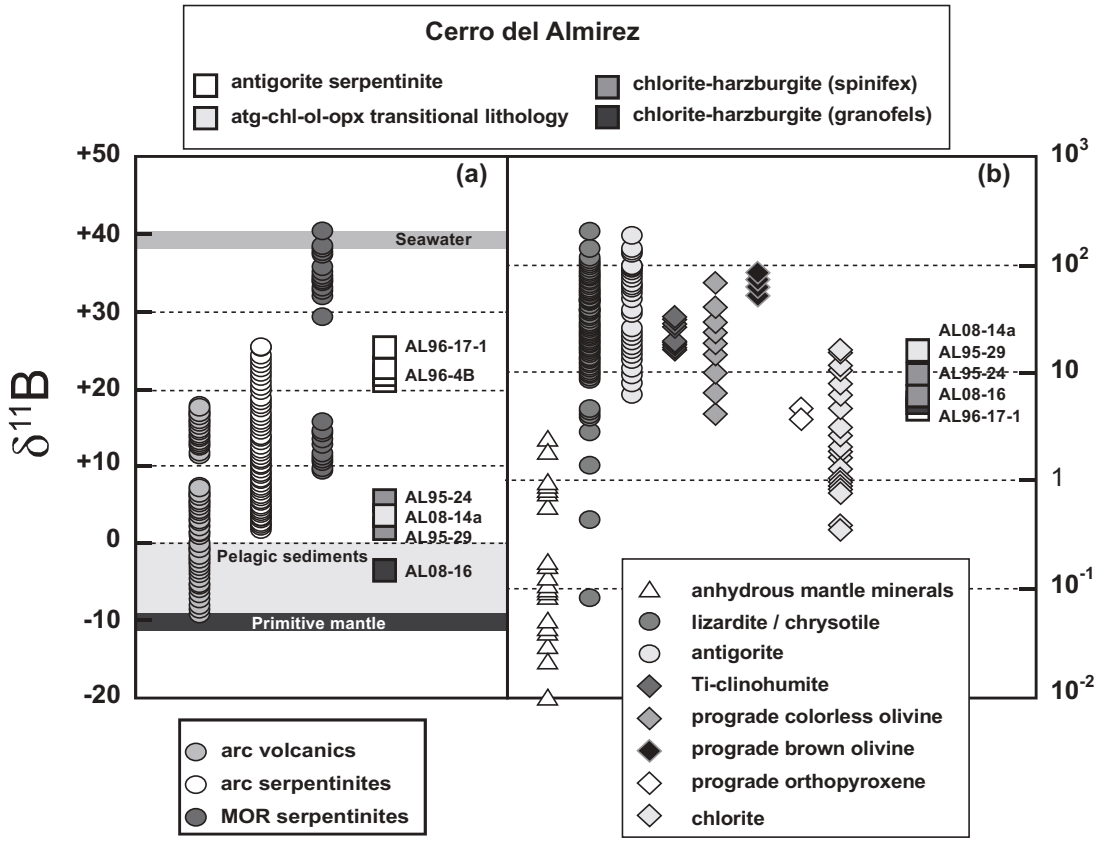

Figure 2.

Table

Click here to download Table: Table 1.doc

Sample	$^{11}B/^{10}B$	+/-	$\delta^{11}B$	+/-	[B]	+/-	$^{87}Sr/^{86}Sr$	+/-	[Sr]
Antigorite-serpentinite									
AL 96-17-1	4.1446	0.0035	22.37	0.86	7.03	0.04	0.70819	0.00001	2.29
AL 96-17-1*	4.1550	0.0068	25.07	1.68					
AL 96-17-1#	4.1410	0.0045	21.61	1.11					
AL 96-4B	4.1450	0.0055	22.60	1.36			0.70871	0.00002	0.33
Transitional lithologies									
AL 08-14a	4.0671	0.0014	3.25	0.35	11.78	0.03	0.70847	0.00003	4.33
AL 08-14a*	4.0671	0.0014	3.38	0.35					
Granofels texture chlorite harzburgite									
AL 08-16	4.0399	0.0011	-3.46	0.27	7.15	0.02	0.70824	0.00004	1.23
AL 08-16*	4.0399	0.0011	-3.33	0.27					
Spinifex texture chlorite harzburgite									
AL 95-29	4.0648	0.0014	2.68	0.35	10.34	0.01	0.70752	0.00001	5.57
AL 95-29*	4.0623	0.0055	2.20	1.36			0.70753	0.00001	5.66
AL 95-29#	4.0648	0.0014	2.81	0.35					
AL 95-24	4.0786	0.0031	6.22	0.76	7.59	0.01	0.70763	0.00001	9.50

Table 1. Boron and strontium elemental abundance and isotope ratios of ultramafic rocks from the Cerro del Almirez. * = duplicate analysis, # triplicate analysis. $\delta^{11}B$ expressed in ‰, elemental abundances expressed in μg g^{-1}. Sample localities for AL95-24, AL95-29 and AL96-17-1 can

be found in Figure 1A of Garrido et al. (2005). Location of samples AL08-14 and AL08-16 are 30S 507457 4104646 and 30S 507639 4104813 respectively, using the ED50 co-ordinate system (European datum 1950), UTM.